AIMS Mathematics, 9(6): 16116–16145.
DOI:10.3934/math.2024780
Received: 15 March 2024
Revised: 22 April 2024
Accepted: 28 April 2024
Published: 08 May 2024

http://www.aimspress.com/journal/Math

Research article

Analysis of bifurcation, chaotic structures, lump and $M-W$-shape soliton solutions to $(2+1)$ complex modified Korteweg-de-Vries system

M. A. El-Shorbagy[1,2], Sonia Akram[3], Mati ur Rahman[4,5,*] and Hossam A. Nabwey[1,2]

[1] Department of Mathematics, College of Science and Humanities in Al-Kharj, Prince Sattam bin Abdulaziz University, Al-Kharj 11942, Saudi Arabia
[2] Department of Basic Engineering Science, Faculty of Engineering, Menoufia University, Shebin El-Kom 32511, Egypt
[3] Department of Mathematics, Faculty of Science, University of Gujrat, Gujrat-50700, Pakistan
[4] School of Mathematical Sciences, Jiangsu University, Zhenjiang 212013, Jiangsu, China
[5] Department of Computer Science and Mathematics, Lebanese American University, Beirut, Lebanon

* **Correspondence:** Email: matimaths@ujs.edu.cn.

Abstract: This research focuses on the fascinating exploration of the (2 + 1)-dimensional complex modified Korteweg-de Vries (CmKdV) system, exhibiting its complex dynamics and solitary wave solutions. This system is a versatile mathematical model that finds applications in various branches of physics, including fluid dynamics, plasma physics, optics, and nonlinear dynamics. Two newly developed methodologies, namely the auxiliary equation (AE) method and the Hirota bilinear (HB) method, are implemented for the construction of novel solitons in various formats. Numerous novel soliton solutions are synthesised in distinct formats, such as dark, bright, singular, periodic, combo, W-shape, mixed trigonometric, exponential, hyperbolic, and rational, based on the proposed methods. Furthermore, we also find some lump solutions, including the periodic cross rational wave, the homoclinic breather (HB) wave solution, the periodic wave solution, the M-shaped rational wave solution, the M-shaped interaction with one kink wave, and the multiwave solution, which are not documented in the literature. In addition, we employ the Galilean transformation to derive the dynamic framework for the presented equation. Our inquiry includes a wide range of topics, including bifurcations, chaotic flows, and other intriguing dynamic properties. Also, for the physical demonstration of the acquired solutions, 3D, 2D, and contour plots are provided. The resulting structure of the acquired results can enrich the nonlinear dynamical behaviors of the given system and may be useful in many domains, such as mathematical physics and fluid dynamics, as well as demonstrate that the approaches used are effective and worthy of validation.

Keywords: soliton solutions; (2+1)-dimensional CmKDV equations; the AE scheme; the HB method;

bifurcation theory; Galilean transformation
Mathematics Subject Classification: 35A09, 35C08

1. Introduction

Nonlinear partial differential equations (PDEs) propose groundwork in the scientific description of complicated manifestations throughout numerous systematic disciplines that play a vital role in providing thoughtful insight into the complex changing aspects of natural systems [1–5]. These equations have emerged as a focal point in contemporary nonlinear research, notably in the study of integrable systems. This research area provides vital insights that enrich our understanding of nonlinear processes in a variety of scientific domains, including plasma physics, fluid dynamics, and nonlinear optics, both of which rely significantly on NLPDEs for practical applications. NLPDEs are an effective tool for characterizing a wide variety of phenomena, including optics, nonlinear fiber optics, plasma physics, engineering, and physical effects in fluid dynamics [6–11]. In recent years, a devoted crew of academics has made major attempts to uncover the qualitative and quantitative aspects of these equations, with a special emphasis on investigating soliton solutions within the context of NLPDEs.

Nonlinear evolution equations (NLEEs) are mathematical equations that describe the evolution of systems where nonlinear interactions play a significant role. These equations arise in various branches of science and engineering, encompassing diverse phenomena such as wave propagation, pattern formation, turbulence, and particle dynamics [12]. They describe how the system evolves in time based on the current state of the system. NLEEs have widespread applications across various fields, including physics, engineering, biology, and finance. They are used to model and understand a wide range of phenomena, including wave propagation, fluid dynamics, chemical reactions, population dynamics, and financial markets [13, 14]. Finding accurate solutions to nonlinear NLEEs is critical in nonlinear systems research because they provide a thorough understanding of the underlying physical processes. For this purpose, researchers and scientists have employed several successful strategies, such as the multiple exponential function method [15], the $(\frac{1}{G'})$-expansion method [16], the new Kudryashov method [17], the improved $\mathcal{F}$-expansion method [18], the sardar sub-equation method [19], the Hirota bilinear method [20], the extended simple method [21], the Heir equation method [22], the first integral equation method [23], the Darboux transformation method [24], and the Nucci reduction method [25, 26], to gain deeper insights into the behavior of complex systems and to refine their understanding of real-world phenomena. Futhermore, by employing the dressing method, Wang et al. [27] successfully deduced the three-component coupled Hirota hierarchy. An effective and direct approach was proposed by Tian et al. [28] to study the symmetry-preserving discretization for a class of generalized higher-order equations, and they proposed an open problem about symmetries and the multipliers of the conservation law. In addition, by using the Riemann-Hilbert method, Li and Tian [29] solved the Cauchy problem of the general n-component nonlinear Schrödinger equations, and gave the N-soliton solutions. Besides, a conjecture about the law of nonlinear wave propagation was proposed. Moreover, by employing the $\bar{D}$-steepest descent method, Li, Tian, Yang, and Fan have done some interesting work with respect to the solutions of the Wadati-Konno-Ichikawa equation and other complex equations [30, 31]. They solved the long-time asymptotic behavior of the solutions of

these equations, and proved the soliton resolution conjecture and the asymptotic stability of solutions of these equations [32].

The CmKDV sytem is a fundamental model in the study of nonlinear waves and fluid dynamics, offering insights into the formation and propagation of coherent structures in various physical systems. The CmKDV system supports soliton solutions, which are localized, stable, nonlinear waves that propagate without dispersion. These solitons are often interpreted as coherent structures in fluid dynamics and can describe phenomena such as rogue waves. In the current study, we consider the (2+1) dimentional CmKDV equation [33], which occurs in several applied science and optics disciplines:

$$\begin{aligned} \mathcal{N}_t + \mathcal{N}_{xxy} + i\mathcal{N}\mathcal{H} + (\mathcal{N}\mathcal{Q})_x = 0.\\ \mathcal{H}_x + 2i\lambda(\mathcal{N}^*\mathcal{N}_{xy} - \mathcal{N}^*_{xy}\mathcal{N}) = 0,\\ \mathcal{Q}_x - 2\lambda(|\mathcal{N}|^2)_y = 0. \end{aligned} \tag{1.1}$$

The function $\mathcal{N}(x, y, t)$ is a complex function with its conjugate denoted as $\mathcal{N}^*(x, y, t)$, and $\mathcal{H}(x, y, t)$ and $\mathcal{Q}(x, y, t)$ are real functions. This model generalizes the (2 + 1)-dimension CmKdV equation and has significant applications in nanomagnetism and ferromagnetism [33]. The Darboux transformation (DT) is used in various works to study Eq (1.1). Starting from zero, the one-soliton and two-soliton solutions are found using DT [34]. Moreover, n-fold DT is used to generate deformed solitons [35]. The plane wave, breather solutions, and periodic line wave solutions were found in [36]. The authors in [37] also established the order-n-breather solutions. The nonlocal counterpart was fully investigated in [38]. Other investigations, via the concept of traveling wave solutions for Eq (1.1), were established by elaborating on the sine-cosine, Kudryashov, and tanh-coth methods [39]. However, the main goal of this study is to investigate the (2 + 1)-dimentional CmKDV equations by using the AE scheme and the HB method. The CmKDV equations are crucial for simulating soliton propagation in mathematical sciences, and the solutions that are produced can be used to explain several significant physical events. Also, bifurcation analysis of the aforementioned model is performed, which is especially essential in dynamical systems. Using the aforementioned approaches, we compare our results to those discovered in [33] and find that the current work contains several innovative solutions. This study has yielded numerous solitary as well as lump solutions which have not been documented in previous literature. In addition, some of the discovered solutions are graphically represented.

The remaining structure of our manuscript is as follows: Section 3 presents the methodology of the selected method. The applications of the selected method are displayed in Section 4. The applications of the HB method are demonstrated in Section 5. The bifurcations and chaotic dynamics are presented in Section 6. The results are illustrated in Section 8. Finally, we provide our concluding remark in Section 9.

2. The Lax pair system of the equation

The Lax pair system of equations for Eq (1.1) is [40]

$$\Pi_x = \mathcal{X}\Pi, \qquad \Pi_t = 4\sigma^2\Pi_y + \mathcal{Z}\Pi, \tag{2.1}$$

where,

$$\mathcal{X} = \sigma\mathcal{J} + \mathcal{X}_0, \qquad \mathcal{Z} = \sigma\mathcal{Z}_1 + \mathcal{Z}_0, \tag{2.2}$$

with,

$$\mathcal{J} = \begin{pmatrix} -i & 0 \\ 0 & i \end{pmatrix}, \quad \mathcal{X}_0 = \begin{pmatrix} 0 & \mathcal{N} \\ -\mathcal{R} & 0 \end{pmatrix}, \quad \mathcal{Z}_1 = \begin{pmatrix} i\mathcal{Q} & 2i\mathcal{N}_y \\ 2i\mathcal{R}_y & -i\mathcal{Q} \end{pmatrix}, \tag{2.3}$$

$$\mathcal{Z}_0 = \begin{pmatrix} -\frac{i\mathcal{H}}{2} & -\mathcal{N}_{xy} - \mathcal{Q}\mathcal{N} \\ \mathcal{R}_{xy} + \mathcal{Q}\mathcal{R} & \frac{i\mathcal{H}}{2} \end{pmatrix}, \quad \Pi = \begin{pmatrix} \Pi_1(\sigma, x, y, t) \\ \Pi_2(\sigma, x, y, t) \end{pmatrix}, \tag{2.4}$$

and the compatibility condition

$$\mathcal{X}_t - \mathcal{Z}_x + \mathcal{X}\mathcal{Z} - \mathcal{Z}\mathcal{X} - 4\sigma^2\mathcal{X}_y = 0. \tag{2.5}$$

This infers the following (2 + 1)-dimensional coupled CmKdV equations:

$$\begin{aligned} \mathcal{N}_t + \mathcal{N}_{xxy} + i\mathcal{N}\mathcal{H} + (\mathcal{Q}\mathcal{N})_x = 0, \\ \mathcal{R}_t + \mathcal{R}_{xxy} - i\mathcal{H}\mathcal{R} + (\mathcal{Q}\mathcal{R})_x = 0, \\ \mathcal{H}_x + 2i(\mathcal{R}\mathcal{N}_{xy} - \mathcal{R}_{xy}\mathcal{N}) = 0, \\ \mathcal{H}_x - 2(\mathcal{N}\mathcal{R})_y = 0 \end{aligned} \tag{2.6}$$

where $\mathcal{H}$, $\mathcal{Q}$ are complex and real functions. By setting $\mathcal{R} = \lambda\mathcal{N}^*$, Eq (2.6) becomes the CmKdV equations (1.1).

3. Methodology

In this section, the procedures employed will be described. We consider a particular type of nonlinear fractional equation given by

$$\mathcal{G}(\mathcal{H},\ \mathcal{H}_x,\ \mathcal{H}_y,\ \mathcal{H}_{xx},\ \mathcal{H}_{xy},\ \mathcal{H}_{xt},\ \mathcal{H}_{yy},\ \cdots) = 0. \tag{3.1}$$

The wave transformation is defined as

$$\mathcal{H}(x, y, t) \ = \ \mathcal{P}(\zeta), \quad \text{where } \zeta = ax + by + cz - \mu t. \tag{3.2}$$

Here, $\mathcal{P}(\zeta)$ denotes the amplitude. In accordance with the strategy, the above transformation changes Eq (3.2) into the nonlinear ordinary differential equation (ODE)

$$\mathcal{Q}(\mathcal{P},\ \mathcal{P}',\ \mathcal{P}'',\ \cdots) = 0. \tag{3.3}$$

3.1. The AE method

This section provides a fresh revision of the AE approach. The revised methodology results in novel and differentiated findings. To achieve various results, we assume a trial solution of Eq (3.3) as the **1st step.** Suppose the trial solution of Eq (3.3) is given by

$$\mathcal{P}(\zeta) = \gamma_0 + \sum_{i=1}^{n} \gamma_i \mathcal{S}(\zeta)^i, \ \gamma_n \neq 0, \tag{3.4}$$

where $\gamma_i (i = 0, 1, 2, \cdots, n)$ should be computed after the constants. Equation (3.4) and the function $\mathcal{S}(\zeta)$ are satisfied by the Ricati equation

$$(\mathcal{S}'(\zeta))^2 = \sqrt{\wp_1 \mathcal{S}(\zeta)^2 + \wp_2 \mathcal{S}(\zeta)^3 + \wp_3 \mathcal{S}(\zeta)^4}. \tag{3.5}$$

where $\wp_0$, $\wp_1$, and $\wp_2$ are parameters. Furthermore, mentioned below are typical solutions to Eq (3.5):

$$\mathcal{S}_1(\zeta) = -\frac{\wp_1 \wp_2 \text{sech}\left(\frac{\sqrt{\wp_1}\zeta}{2}\right)^2}{\wp_2^2 - \wp_3 \wp_1 \left(\varepsilon \tanh\left(\frac{\sqrt{\wp_1}\zeta}{2}\right) + 1\right)^2}, \ \wp_1 > 0, \tag{3.6}$$

$$\mathcal{S}_2(\zeta) = \frac{\wp_1 \wp_2 \text{csch}\left(\frac{\sqrt{\wp_1}\zeta}{2}\right)^2}{\wp_2^2 - \wp_3 \wp_1 \left(\varepsilon \coth\left(\frac{\sqrt{\wp_1}\zeta}{2}\right) + 1\right)^2}, \ \wp_1 > 0, \tag{3.7}$$

$$\mathcal{S}_3(\zeta) = \frac{2\wp_1 \text{sech}\left(\sqrt{\wp_1}\zeta\right)}{\varepsilon\sqrt{\Omega} - \wp_2 \text{sech}\left(\sqrt{\wp_1}\zeta\right)}, \ \wp_1 > 0 \ \textit{and} \ \Omega > 0, \tag{3.8}$$

$$\mathcal{S}_4(\zeta) = \frac{2\wp_1 \sec\left(\sqrt{-\wp_1}\zeta\right)}{\varepsilon\sqrt{\Omega} - \wp_2 \sec\left(\sqrt{-\wp_1}\zeta\right)}, \ \wp_1 < 0, \ \Omega > 0, \tag{3.9}$$

$$\mathcal{S}_5(\zeta) = \frac{2\wp_1 \text{csch}\left(\sqrt{\wp_1}\zeta\right)}{\varepsilon\sqrt{-\Omega} - \wp_2 \text{csch}\left(\frac{\sqrt{\wp_1}\zeta}{2}\right)}, \ \wp_1 > 0, \ \Omega < 0. \tag{3.10}$$

$$\mathcal{S}_6(\zeta) = \frac{2\wp_1 \csc\left(\sqrt{-\wp_1}\zeta\right)}{\varepsilon\sqrt{\Omega} - \wp_2 \csc\left(\sqrt{-\wp_1}\zeta\right)}, \ \wp_1 < 0, \ \Omega > 0, \tag{3.11}$$

$$\mathcal{S}_7(\zeta) = -\frac{\wp_1 \text{sech}^2\left(\frac{\sqrt{\wp_1}\zeta}{2}\right)}{\wp_2 + 2\sqrt{-\wp_1 \wp_3}\varepsilon \tanh\left(\frac{\sqrt{\wp_1}\zeta}{2}\right)}, \ \wp_1 > 0, \wp_2 > 0, \tag{3.12}$$

$$\mathcal{S}_8(\zeta) = -\frac{\wp_1 \sec^2\left(\frac{1}{2}\sqrt{-\wp_1}\zeta\right)}{\wp_2 + 2\sqrt{-\wp_1 \wp_3}\varepsilon \tan\left(\frac{1}{2}\sqrt{-\wp_1}\zeta\right)}, \ \wp_1 < 0, \wp_2 > 0, \tag{3.13}$$

$$\mathcal{S}_9(\xi) = \frac{\wp_1 \text{csch}^2\left(\frac{1}{2}\sqrt{-\wp_1}\zeta\right)}{\wp_2 + 2\sqrt{\wp_1 \wp_3}\varepsilon \coth\left(\frac{1}{2}\sqrt{-\wp_1}\zeta\right)}, \ \wp_1 > 0, \wp_2 > 0, \tag{3.14}$$

$$\mathcal{S}_{10}(\zeta) = -\frac{\wp_1 \csc^2\left(\frac{1}{2}\sqrt{-\wp_1}\zeta\right)}{\wp_2 + 2\sqrt{-\wp_1\wp_3}\varepsilon\cot\left(\frac{1}{2}\sqrt{-\wp_1}\zeta\right)},\ \wp_1 < 0, \gamma_2 > 0, \tag{3.15}$$

$$\mathcal{S}_{11}(\zeta) = -\frac{\wp_1\left(\varepsilon\tanh^2\left(\frac{\sqrt{\wp_1}\zeta}{2}\right)+1\right)}{\wp_2},\ \wp_1 > 0,\ \Omega = 0, \tag{3.16}$$

$$\mathcal{S}_{12}(\zeta) = -\frac{\wp_1\left(\varepsilon\coth^2\left(\frac{\sqrt{\wp_1}\zeta}{2}\right)+1\right)}{\wp_2},\ \wp_1 > 0,\ \Omega = 0, \tag{3.17}$$

$$\mathcal{S}_{13}(\zeta) = \frac{4\wp_1\exp\left(e\left(\sqrt{\wp_1}\zeta\right)\right)}{\exp^2\left(\varepsilon\left(\sqrt{\wp_1}\zeta\right)-\wp_2\right)-4\wp_3\wp_1},\ \wp_1 > 0, \tag{3.18}$$

Where, $\Omega = \wp_2^2 - 4\wp_3\wp_1$ and $\varepsilon = \pm 1$ is parameter.

2nd step. We calculate the value of n by applying balance theory on Eq (3.3).

3rd step. Substituting Eqs (3.4) and (3.5) into Eq (3.3), and setting all the coefficients power of $\mathcal{S}(\zeta)$ to zero. Finally, by using computational software, we solve these equations to obtain the values of the unknowns $\gamma_0,\ \gamma_i$, and μ, which will be utilized to obtain the solution of Eq (3.1).

4. Extraction of solution

The major goal of this part is to compile a diverse set of solutions to the given model. Now, by using the complex wave transformations, we have

$$\mathcal{N}(x,y,t) \quad = \quad \mathcal{P}(\zeta)e^{i\psi}(x,t), \tag{4.1}$$

where $\zeta = ax + by + \mu t$ and $\psi = \kappa_1 x + \kappa_2 y + \kappa_3 t$.

The function $\mathcal{P}(\zeta)$ illustrates the amplitude component. The unknowns $\kappa_1,\ \kappa_2,\ \kappa_3$, and μ represent independent variables. Substituting Eq (4.1) into Eq (1.1), we get

$$\mathcal{P}_t - 2\kappa_1\kappa_2\mathcal{P}_x - \kappa_1^2\mathcal{P}_y + \mathcal{P}_{xxy} + \mathcal{P}_x\mathcal{Q} + \mathcal{P}\mathcal{Q}_x + i((\kappa_3 - \kappa_1^2\kappa_2)\mathcal{P} + 2\kappa_1\mathcal{P}_{xy} + \kappa_2\mathcal{P}_{xx} + \kappa_1\mathcal{P}\mathcal{Q} + \mathcal{P}\mathcal{H} = 0. \tag{4.2}$$

$$\mathcal{H}_x - 4\lambda(\kappa_2\mathcal{P}\mathcal{P}_x + \kappa_1\mathcal{P}\mathcal{P}_y = 0, \tag{4.3}$$

$$\mathcal{Q}_x - 2\lambda(\mathcal{P}^2)_y = 0. \tag{4.4}$$

Substituting the wave transformation

$$\mathcal{N}(x,y,t) = \mathcal{P}(\zeta) = \mathcal{P}(x+y+\mu t), \tag{4.5}$$

$$\mathcal{H}(x,y,t) = \mathcal{H}(\zeta) = \mathcal{H}(x+y+\mu t), \tag{4.6}$$

$$\mathcal{Q}(x,y,t) = \mathcal{Q}(\zeta) = \mathcal{Q}(x+y+\mu t), \tag{4.7}$$

into system (4.3) and (4.4), we get,

$$(\mu - 2\kappa_1\kappa_2 - \kappa_1^2)\mathcal{P}' + \mathcal{P}''' + \mathcal{P}'\mathcal{Q} + \mathcal{P}\mathcal{Q}' + i((\kappa_3 - \kappa_1^2\kappa_2)\mathcal{P} + (2\kappa_1 + \kappa_2)\mathcal{P}'' + \kappa_1\mathcal{N}\mathcal{Q} + \mathcal{P}\mathcal{Q}) = 0, \tag{4.8}$$

$$\mathcal{H}^{'} - 4\lambda(\kappa_2 + \kappa_1)\mathcal{P}\mathcal{P}^{'} = 0, \quad (4.9)$$

$$\mathcal{Q}^{'} - 2\lambda(\mathcal{P}^2)^{'} = 0. \quad (4.10)$$

Integrating Eqs (4.9) and (4.10) with respect to ζ and taking the integration constant as zero, we have

$$\mathcal{H} = 2\lambda(\kappa_2 + \kappa_1)\mathcal{P}^2, \qquad \mathcal{Q} = 2\lambda\mathcal{P}^2. \quad (4.11)$$

Substituting Eq (4.11) into Eq (4.9), we get the following ODE:

$$(\mu - 2\kappa_1\kappa_2 - \kappa_1^2)\mathcal{P}^{'} + \mathcal{P}^{'''} + 2\lambda(\mathcal{P}^3)^{'} + i((\kappa_3 - \kappa_1^2\kappa_2)\mathcal{P} + (2\kappa_1 + \kappa_2)\mathcal{P}^{''} + 2\lambda(2\kappa_1 + \kappa_2)\mathcal{P}^3) = 0. \quad (4.12)$$

Now, splitting the real and imaginary parts of Eq (4.12), we have

$$(\mu - 2\kappa_1\kappa_2 - \kappa_1^2)\mathcal{P}^{'} + \mathcal{P}^{'''} + 2\lambda(\mathcal{P}^3)^{'} = 0, \quad (4.13)$$

$$\frac{(\kappa_3 - \kappa_1^2\kappa_2)}{(2\kappa_1 + \kappa_2)}\mathcal{P} + \mathcal{P}^{''} + 2\lambda\mathcal{P}^3 = 0. \quad (4.14)$$

Taking the anti-derivative of Eq (4.14) once with respect to ζ, and setting the constant of integration to zero, we have

$$(\mu - 2\kappa_1\kappa_2 - \kappa_1^2)\mathcal{P} + \mathcal{P}^{''} + 2\lambda(\mathcal{P}^3) = 0. \quad (4.15)$$

Equations (4.14) and (4.15) are the same if and only if the following constraint condition is satisfied:

$$\mu - 2\kappa_1\kappa_2 - \kappa_1^2 = \frac{\kappa_3 - \kappa_1^2\kappa_2}{2\kappa_1 - \kappa_2}. \quad (4.16)$$

Solving for

$$\mu = 2\kappa_1\kappa_2 + \kappa_1^2 + \frac{\kappa_3 - \kappa_1^2\kappa_2}{2\kappa_1 - \kappa_2}, \quad (4.17)$$

we rewrite Eq (4.14) as

$$\mathcal{P}^{''} + \frac{\kappa_3 - \kappa_1^2\kappa_2}{2\kappa_1 - \kappa_2}\mathcal{P} + 2\lambda\mathcal{P}^3 = 0. \quad (4.18)$$

4.1. Application of the AE method

In Eq (4.18), we get $N = 1$ by balancing the highest power nonlinear term $\mathcal{P}^3$ with the largest derivative $\mathcal{P}^{''}$. Then, from Eq (3.4), we get

$$\mathcal{P}(\zeta) = \gamma_0 + \gamma_1\mathcal{S}(\zeta). \quad (4.19)$$

Inserting Eqs (4.19) and (3.5) into Eq (4.18) yields a system of algebraic equations. By solving them, we determine the following solution set:

Family-1:

$$\left\{\gamma_0 \to \gamma_0,\ \gamma_1 \to \frac{4\gamma_0\wp_3}{\wp_2},\ \kappa_1 \to -\frac{\sqrt[3]{\kappa_3}}{\sqrt[3]{2}},\ \kappa_2 \to 2^{2/3}\sqrt[3]{\kappa_3},\ \lambda \to -\frac{\wp_2^2}{16\gamma_0^2\wp_3}\right\}. \quad (4.20)$$

Inserting these solutions into Eq (4.19), we recovered the following solutions for the (2 + 1) CmKdV system.

Cluster 1:

$$\mathcal{N}^{\pm}_{1,1}(x,y,t) = \left[\gamma_0\left(1-\frac{4\wp_1\wp_3\mathrm{sech}\left(\frac{1}{2}\sqrt{\wp_1}(+\mu t+x+y)\right)}{\wp_2^2-\wp_1\wp_3\left(\varepsilon\tanh\left(\frac{1}{2}\sqrt{\wp_1}(+\mu t+x+y)\right)+1\right)^2}\right)\right]\times e^{i\kappa_3 t-\frac{i\sqrt[3]{\kappa_3}(x-2y)}{\sqrt[3]{2}}}. \tag{4.21}$$

$$\mathcal{H}^{\pm}_{1,1}(x,y,t) = 2\lambda(\kappa_2+\kappa_1)\times\left[\gamma_0\left(1-\frac{4\wp_1\wp_3\mathrm{sech}\left(\frac{1}{2}\sqrt{\wp_1}(+\mu t+x+y)\right)}{\wp_2^2-\wp_1\wp_3\left(\varepsilon\tanh\left(\frac{1}{2}\sqrt{\wp_1}(+\mu t+x+y)\right)+1\right)^2}\right)\right]^2. \tag{4.22}$$

$$\mathcal{Q}^{\pm}_{1,1}(x,y,t) = 2\lambda\times\left[\gamma_0\left(1-\frac{4\wp_1\wp_3\mathrm{sech}\left(\frac{1}{2}\sqrt{\wp_1}(+\mu t+x+y)\right)}{\wp_2^2-\wp_1\wp_3\left(\varepsilon\tanh\left(\frac{1}{2}\sqrt{\wp_1}(+\mu t+x+y)\right)+1\right)^2}\right)\right]^2. \tag{4.23}$$

Cluster 2:

$$\mathcal{N}^{\pm}_{1,2}(x,y,t) = \left[\gamma_0\left(\frac{4\wp_1\wp_3\mathrm{csch}^2\left(\frac{1}{2}\sqrt{\wp_1}(+\mu t+x+y)\right)}{\wp_2^2-\wp_1\wp_3\left(\varepsilon\coth\left(\frac{1}{2}\sqrt{\wp_1}(+\mu t+x+y)\right)+1\right)^2}+1\right)\right]\times e^{i\kappa_3 t-\frac{i\sqrt[3]{\kappa_3}(x-2y)}{\sqrt[3]{2}}}. \tag{4.24}$$

$$\mathcal{H}^{\pm}_{1,2}(x,y,t) = 2\lambda(\kappa_2+\kappa_1)\times\left[\gamma_0\left(\frac{4\wp_1\wp_3\mathrm{csch}^2\left(\frac{1}{2}\sqrt{\wp_1}(+\mu t+x+y)\right)}{\wp_2^2-\wp_1\wp_3\left(\varepsilon\coth\left(\frac{1}{2}\sqrt{\wp_1}(+\mu t+x+y)\right)+1\right)^2}+1\right)\right]^2. \tag{4.25}$$

$$\mathcal{Q}^{\pm}_{1,2}(x,y,t) = 2\lambda\times\left[\gamma_0\left(\frac{4\wp_1\wp_3\mathrm{csch}^2\left(\frac{1}{2}\sqrt{\wp_1}(+\mu t+x+y)\right)}{\wp_2^2-\wp_1\wp_3\left(\varepsilon\coth\left(\frac{1}{2}\sqrt{\wp_1}(+\mu t+x+y)\right)+1\right)^2}+1\right)\right]^2. \tag{4.26}$$

Cluster 3:

$$\mathcal{N}^{\pm}_{1,3}(x,y,t) = \left[\gamma_0\left(\frac{8\wp_1\wp_3}{\varepsilon\sqrt{\Omega}\wp_2\cosh\left(\sqrt{\wp_1}(+\mu t+x+y)\right)-\wp_2^2}+1\right)\right]\times e^{i\kappa_3 t-\frac{i\sqrt[3]{\kappa_3}(x-2y)}{\sqrt[3]{2}}}. \tag{4.27}$$

$$\mathcal{H}^{\pm}_{1,3}(x,y,t) = 2\lambda(\kappa_2+\kappa_1)\times\left[\gamma_0\left(\frac{8\wp_1\wp_3}{\varepsilon\sqrt{\Omega}\wp_2\cosh\left(\sqrt{\wp_1}(+\mu t+x+y)\right)-\wp_2^2}+1\right)\right]^2. \tag{4.28}$$

$$\mathcal{Q}^{\pm}_{1,3}(x,y,t) = 2\lambda\times\left[\gamma_0\left(\frac{8\wp_1\wp_3}{\varepsilon\sqrt{\Omega}\wp_2\cosh\left(\sqrt{\wp_1}(+\mu t+x+y)\right)-\wp_2^2}+1\right)\right]^2. \tag{4.29}$$

Cluster 4:

$$\mathcal{N}^{\pm}_{1,4}(x,y,t) = \left[\gamma_0\left(\frac{8\wp_1\wp_3}{\varepsilon\sqrt{\Omega}\wp_2\cos\left(\sqrt{-\wp_1}(+\mu t+x+y)\right)-\wp_2^2}+1\right)\right]\times e^{i\kappa_3 t-\frac{i\sqrt[3]{\kappa_3}(x-2y)}{\sqrt[3]{2}}}. \tag{4.30}$$

$$\mathcal{H}^{\pm}_{1,4}(x,y,t) = 2\lambda(\kappa_2+\kappa_1)\times\left[\gamma_0\left(\frac{8\wp_1\wp_3}{\varepsilon\sqrt{\Omega}\wp_2\cos\left(\sqrt{-\wp_1}(+\mu t+x+y)\right)-\wp_2^2}+1\right)\right]^2. \tag{4.31}$$

$$\mathcal{Q}^{\pm}_{1,4}(x,y,t) = 2\lambda\times\left[\gamma_0\left(\frac{8\wp_1\wp_3}{\varepsilon\sqrt{\Omega}\wp_2\cos\left(\sqrt{-\wp_1}(+\mu t+x+y)\right)-\wp_2^2}+1\right)\right]^2. \tag{4.32}$$

Cluster 5:

$$\mathcal{N}^{\pm}_{1,5}(x,y,t) = \left[\gamma_0\left(\frac{8\wp_1\wp_3\mathrm{csch}\left(\sqrt{\wp_1}(+\mu t+x+y)\right)}{\varepsilon\sqrt{-\Omega}\wp_2-\wp_2^2\mathrm{csch}\left(\frac{1}{2}\sqrt{\wp_1}(+\mu t+x+y)\right)}+1\right)\right]\times e^{i\kappa_3 t-\frac{i\sqrt[3]{\kappa_3}(x-2y)}{\sqrt[3]{2}}}. \tag{4.33}$$

$$\mathcal{H}^{\pm}_{1,5}(x,y,t) = 2\lambda(\kappa_2+\kappa_1)\times\left[\gamma_0\left(\frac{8\wp_1\wp_3\mathrm{csch}\left(\sqrt{\wp_1}(+\mu t+x+y)\right)}{\varepsilon\sqrt{-\Omega}\wp_2-\wp_2^2\mathrm{csch}\left(\frac{1}{2}\sqrt{\wp_1}(+\mu t+x+y)\right)}+1\right)\right]^2. \tag{4.34}$$

$$Q^{\pm}_{1,5}(x,y,t) = 2\lambda\times\left[\gamma_0\left(\frac{8\wp_1\wp_3\text{csch}\left(\sqrt{\wp_1}(+\mu t+x+y)\right)}{\varepsilon\sqrt{-\Omega}\wp_2-\wp_2^2\text{csch}\left(\frac{1}{2}\sqrt{\wp_1}(+\mu t+x+y)\right)}+1\right)\right]^2. \tag{4.35}$$

Cluster 6:

$$\mathcal{N}^{\pm}_{1,6}(x,y,t) = \left[\gamma_0\left(\frac{8\wp_1\wp_3}{\varepsilon\sqrt{\Omega}\wp_2\sin\left(\sqrt{-\wp_1}(+\mu t+x+y)\right)-\wp_2^2}+1\right)\right]\times e^{i\kappa_3 t-\frac{i\sqrt[3]{\kappa_3}(x-2y)}{\sqrt[3]{2}}}. \tag{4.36}$$

$$\mathcal{H}^{\pm}_{1,6}(x,y,t) = 2\lambda(\kappa_2+\kappa_1)\times\left[\gamma_0\left(\frac{8\wp_1\wp_3}{\varepsilon\sqrt{\Omega}\wp_2\sin\left(\sqrt{-\wp_1}(+\mu t+x+y)\right)-\wp_2^2}+1\right)\right]^2. \tag{4.37}$$

$$Q^{\pm}_{1,6}(x,y,t) = 2\lambda\times\left[\gamma_0\left(\frac{8\wp_1\wp_3}{\varepsilon\sqrt{\Omega}\wp_2\sin\left(\sqrt{-\wp_1}(+\mu t+x+y)\right)-\wp_2^2}+1\right)\right]^2. \tag{4.38}$$

Cluster 7:

$$\mathcal{N}^{\pm}_{1,7}(x,y,t) = \left[\gamma_0\left(1-\frac{4\wp_1\wp_3\text{sech}^2\left(\frac{1}{2}\sqrt{\wp_1}(+\mu t+x+y)\right)}{2\varepsilon\sqrt{-\wp_1\wp_3}\wp_2\tanh\left(\frac{1}{2}\sqrt{\wp_1}(+\mu t+x+y)\right)+\wp_2^2}\right)\right]\times e^{i\kappa_3 t-\frac{i\sqrt[3]{\kappa_3}(x-2y)}{\sqrt[3]{2}}}. \tag{4.39}$$

$$\mathcal{H}^{\pm}_{1,7}(x,y,t) = 2\lambda(\kappa_2+\kappa_1)\times\left[\gamma_0\left(1-\frac{4\wp_1\wp_3\text{sech}^2\left(\frac{1}{2}\sqrt{\wp_1}(+\mu t+x+y)\right)}{2\varepsilon\sqrt{-\wp_1\wp_3}\wp_2\tanh\left(\frac{1}{2}\sqrt{\wp_1}(+\mu t+x+y)\right)+\wp_2^2}\right)\right]^2. \tag{4.40}$$

$$Q^{\pm}_{1,7}(x,y,t) = 2\lambda\times\left[\gamma_0\left(1-\frac{4\wp_1\wp_3\text{sech}^2\left(\frac{1}{2}\sqrt{\wp_1}(+\mu t+x+y)\right)}{2\varepsilon\sqrt{-\wp_1\wp_3}\wp_2\tanh\left(\frac{1}{2}\sqrt{\wp_1}(+\mu t+x+y)\right)+\wp_2^2}\right)\right]^2. \tag{4.41}$$

Cluster 8:

$$\mathcal{N}^{\pm}_{1,8}(x,y,t) = \left[\gamma_0\left(1-\frac{4\wp_1\wp_3\sec^2\left(\frac{1}{2}\sqrt{-\wp_1}(+\mu t+x+y)\right)}{2\varepsilon\sqrt{-\wp_1\wp_3}\wp_2\tan\left(\frac{1}{2}\sqrt{-\wp_1}(+\mu t+x+y)\right)+\wp_2^2}\right)\right]\times e^{i\kappa_3 t-\frac{i\sqrt[3]{\kappa_3}(x-2y)}{\sqrt[3]{2}}}. \tag{4.42}$$

$$\mathcal{H}^{\pm}_{1,8}(x,y,t) = 2\lambda(\kappa_2+\kappa_1)\times\left[\gamma_0\left(1-\frac{4\wp_1\wp_3\sec^2\left(\frac{1}{2}\sqrt{-\wp_1}(+\mu t+x+y)\right)}{2\varepsilon\sqrt{-\wp_1\wp_3}\wp_2\tan\left(\frac{1}{2}\sqrt{-\wp_1}(+\mu t+x+y)\right)+\wp_2^2}\right)\right]^2. \tag{4.43}$$

$$Q^{\pm}_{1,8}(x,y,t) = 2\lambda\times\left[\gamma_0\left(1-\frac{4\wp_1\wp_3\sec^2\left(\frac{1}{2}\sqrt{-\wp_1}(+\mu t+x+y)\right)}{2\varepsilon\sqrt{-\wp_1\wp_3}\wp_2\tan\left(\frac{1}{2}\sqrt{-\wp_1}(+\mu t+x+y)\right)+\wp_2^2}\right)\right]^2. \tag{4.44}$$

Cluster 9:

$$\mathcal{N}^{\pm}_{1,9}(x,y,t) = \left[\gamma_0\left(\frac{4\wp_1\wp_3\text{csch}^2\left(\frac{1}{2}\sqrt{-\wp_1}(+\mu t+x+y)\right)}{2\varepsilon\sqrt{\wp_1\wp_3}\wp_2\coth\left(\sqrt{-\frac{\gamma_0\wp_3}{\wp_2}}(+\mu t+x+y)\right)+\wp_2^2}+1\right)\right]\times e^{i\kappa_3 t-\frac{i\sqrt[3]{\kappa_3}(x-2y)}{\sqrt[3]{2}}}. \tag{4.45}$$

$$\mathcal{H}^{\pm}_{1,9}(x,y,t) = 2\lambda(\kappa_2+\kappa_1)\times\left[\gamma_0\left(\frac{4\wp_1\wp_3\text{csch}^2\left(\frac{1}{2}\sqrt{-\wp_1}(+\mu t+x+y)\right)}{2\varepsilon\sqrt{\wp_1\wp_3}\wp_2\coth\left(\sqrt{-\frac{\gamma_0\wp_3}{\wp_2}}(+\mu t+x+y)\right)+\wp_2^2}+1\right)\right]^2. \tag{4.46}$$

$$Q^{\pm}_{1,9}(x,y,t) = 2\lambda\times\left[\gamma_0\left(\frac{4\wp_1\wp_3\text{csch}^2\left(\frac{1}{2}\sqrt{-\wp_1}(+\mu t+x+y)\right)}{2\varepsilon\sqrt{\wp_1\wp_3}\wp_2\coth\left(\sqrt{-\frac{\gamma_0\wp_3}{\wp_2}}(+\mu t+x+y)\right)+\wp_2^2}+1\right)\right]^2. \tag{4.47}$$

Cluster 10:

$$\mathcal{N}^{\pm}_{1,10}(x,y,t) = \left[\gamma_0\left(1-\frac{4\wp_1\wp_3\csc^2\left(\frac{1}{2}\sqrt{-\wp_1}(+\mu t+x+y)\right)}{2\varepsilon\sqrt{-\wp_1\wp_3}\wp_2\cot\left(\frac{1}{2}\sqrt{-\wp_1}(+\mu t+x+y)\right)+\wp_2^2}\right)\right]\times e^{i\kappa_3 t-\frac{i\sqrt[3]{\kappa_3}(x-2y)}{\sqrt[3]{2}}}. \tag{4.48}$$

$$\mathcal{H}^{\pm}_{1,10}(x,y,t) = 2\lambda(\kappa_2+\kappa_1)\times\left[\gamma_0\left(1-\frac{4\wp_1\wp_3\csc^2\left(\frac{1}{2}\sqrt{-\wp_1}(+\mu t+x+y)\right)}{2\varepsilon\sqrt{-\wp_1\wp_3}\wp_2\cot\left(\frac{1}{2}\sqrt{-\wp_1}(+\mu t+x+y)\right)+\wp_2^2}\right)\right]^2. \tag{4.49}$$

$$Q^{\pm}_{1,10}(x,y,t) = 2\lambda\times\left[\gamma_0\left(1-\frac{4\wp_1\wp_3\csc^2\left(\frac{1}{2}\sqrt{-\wp_1}(+\mu t+x+y)\right)}{2\varepsilon\sqrt{-\wp_1\wp_3}\wp_2\cot\left(\frac{1}{2}\sqrt{-\wp_1}(+\mu t+x+y)\right)+\wp_2^2}\right)\right]^2. \tag{4.50}$$

Cluster 11:

$$\mathcal{N}^{\pm}_{1,11}(x,y,t) = \left[\frac{\gamma_0\left(\wp_2^2-4\wp_1\wp_3\left(\varepsilon\tanh^2\left(\frac{1}{2}\sqrt{\wp_1}(+\mu t+x+y)\right)+1\right)\right)}{\wp_2^2}\right]\times e^{ik_3t-\frac{i\sqrt[3]{\kappa_3}(x-2y)}{\sqrt[3]{2}}}. \tag{4.51}$$

$$\mathcal{H}^{\pm}_{1,11}(x,y,t) = 2\lambda(\kappa_2+\kappa_1)\times\left[\frac{\gamma_0\left(\wp_2^2-4\wp_1\wp_3\left(\varepsilon\tanh^2\left(\frac{1}{2}\sqrt{\wp_1}(+\mu t+x+y)\right)+1\right)\right)}{\wp_2^2}\right]^2. \tag{4.52}$$

$$Q^{\pm}_{1,11}(x,y,t) = 2\lambda\times\left[\frac{\gamma_0\left(\wp_2^2-4\wp_1\wp_3\left(\varepsilon\tanh^2\left(\frac{1}{2}\sqrt{\wp_1}(+\mu t+x+y)\right)+1\right)\right)}{\wp_2^2}\right]^2. \tag{4.53}$$

Cluster 12:

$$\mathcal{N}^{\pm}_{1,12}(x,y,t) = \left[\frac{\gamma_0\left(\wp_2^2-4\wp_1\wp_3\left(\varepsilon\coth^2\left(\frac{1}{2}\sqrt{\wp_1}(+\mu t+x+y)\right)+1\right)\right)}{\wp_2^2}\right]\times e^{ik_3t-\frac{i\sqrt[3]{\kappa_3}(x-2y)}{\sqrt[3]{2}}}. \tag{4.54}$$

$$\mathcal{H}^{\pm}_{1,12}(x,y,t) = 2\lambda(\kappa_2+\kappa_1)\times\left[\frac{\gamma_0\left(\wp_2^2-4\wp_1\wp_3\left(\varepsilon\coth^2\left(\frac{1}{2}\sqrt{\wp_1}(+\mu t+x+y)\right)+1\right)\right)}{\wp_2^2}\right].^2 \tag{4.55}$$

$$Q^{\pm}_{1,12}(x,y,t) = 2\lambda\times\left[\frac{\gamma_0\left(\wp_2^2-4\wp_1\wp_3\left(\varepsilon\coth^2\left(\frac{1}{2}\sqrt{\wp_1}(+\mu t+x+y)\right)+1\right)\right)}{\wp_2^2}\right]^2. \tag{4.56}$$

Cluster 13:

$$\mathcal{N}^{\pm}_{1,13}(x,y,t) = \left[\gamma_0\left(\frac{16\wp_1\wp_3e^{\varepsilon\sqrt{\wp_1}(+\mu t+x+y)}}{\wp_2\left(e^{2\varepsilon\sqrt{\wp_1}(+\mu t+x+y)-2\wp_2}-4\wp_1\wp_3\right)}+1\right)\right]\times e^{ik_3t-\frac{i\sqrt[3]{\kappa_3}(x-2y)}{\sqrt[3]{2}}}. \tag{4.57}$$

$$\mathcal{H}^{\pm}_{1,13}(x,y,t) = 2\lambda(\kappa_2+\kappa_1)\times\left[\gamma_0\left(\frac{16\wp_1\wp_3e^{\varepsilon\sqrt{\wp_1}(+\mu t+x+y)}}{\wp_2\left(e^{2\varepsilon\sqrt{\wp_1}(+\mu t+x+y)-2\wp_2}-4\wp_1\wp_3\right)}+1\right)\right]^2. \tag{4.58}$$

$$Q^{\pm}_{1,13}(x,y,t) = 2\lambda\times\left[\gamma_0\left(\frac{16\wp_1\wp_3e^{\varepsilon\sqrt{\wp_1}(+\mu t+x+y)}}{\wp_2\left(e^{2\varepsilon\sqrt{\wp_1}(+\mu t+x+y)-2\wp_2}-4\wp_1\wp_3\right)}+1\right)\right]^2. \tag{4.59}$$

5. Extraction of lump soliton solutions

By utilizing the logarithmic transformation in Eq (4.18)

$$\mathcal{P} = 2(lnf)_\zeta, \tag{5.1}$$

equation (5.1) converts Eq (4.18) into a bilinear form as

$$4(2\kappa_1+\kappa_2)(4\lambda+1)f'(\zeta)^3+2f(\zeta)^2\left(2\kappa_1f^{(3)}(\zeta)+\kappa_2f^{(3)}(\zeta)-\kappa_1^2\kappa_2f'(\zeta)+\kappa_3f'(\zeta)\right)-6(2\kappa_1+\kappa_2)f(\zeta)f'(\zeta)f''(\zeta)=0. \tag{5.2}$$

5.1. Periodic cross rational wave

We consider the following test function for extracting the periodic cross rational wave:

$$f = \beta_0 \cos(\alpha_1\zeta + \alpha_2) + \beta_1 \cosh(\alpha_3\zeta + \alpha_4) + (\zeta\varpi_1 + \varpi_2)^2 + (\zeta\varpi_3 + \varpi_4)^2 + \varpi_5, \tag{5.3}$$

where $\alpha_i (i = 1, 2, \cdots, 4)$ and $\varpi_i,\ i = 1, 2, \cdots, 4$ are constants. Inserting Eqs (5.3) into (5.2) and taking coefficients hyperbolic and trigonometric functions to zero with similar powers and hence on proceeding with mathematica, we get

Set-1. When

$$\left\{\alpha_1 \to 0,\ \varpi_1 \to -\frac{\varpi_3\varpi_4}{\varpi_2},\ \kappa_1 \to -\frac{\sqrt[3]{\kappa_3}}{\sqrt[3]{2}},\ \kappa_2 \to 2^{2/3}\sqrt[3]{\kappa_3}\right\}, \tag{5.4}$$

via the above values, we get

$$f = \beta_1 \cosh(\alpha_3\zeta + \alpha_4) + \beta_0 \cos(\alpha_2) + \left(\varpi_2 - \frac{\zeta\varpi_3\varpi_4}{\varpi_2}\right)^2 + (\zeta\varpi_3 + \varpi_4)^2 + \varpi_5. \tag{5.5}$$

Thus,

$$\mathcal{P} = \frac{2\left(\alpha_3\beta_1 \sinh(\alpha_3\zeta + \alpha_4) + \frac{2\zeta\left(\varpi_2^2+\varpi_4^2\right)\varpi_3^2}{\varpi_2^2}\right)}{\beta_1 \cosh(\alpha_3\zeta + \alpha_4) + \beta_0 \cos(\alpha_2) + \left(\varpi_2 - \frac{\zeta\varpi_3\varpi_4}{\varpi_2}\right)^2 + (\zeta\varpi_3 + \varpi_4)^2 + \varpi_5}, \tag{5.6}$$

and by imposing Eq (5.6), we get the following solutions:

Cluster 1:

$$\mathcal{N}^{\pm}_{1,1}(x,y,t) = \left[\frac{2\left(\alpha_3\beta_1 \sinh(\alpha_4 + \alpha_3(+\mu t + x + y)) + \frac{2\left(\varpi_2^2+\varpi_4^2\right)\varpi_3^2(+\mu t+x+y)}{\varpi_2^2}\right)}{\beta_0 \cos(\alpha_2) + \beta_1 \cosh(\alpha_4 + \alpha_3(+\mu t + x + y)) + \left(\varpi_2 - \frac{\varpi_3\varpi_4(+\mu t+x+y)}{\varpi_2}\right)^2 + (\varpi_3(+\mu t + x + y) + \varpi_4)^2 + \varpi_5}\right] \times e^{i\kappa_3 t - \frac{i\sqrt[3]{\kappa_3}(x-2y)}{\sqrt[3]{2}}}. \tag{5.7}$$

$$\mathcal{H}^{\pm}_{1,1}(x,y,t) = 2\lambda(\kappa_2 + \kappa_1) \times \left[\frac{2\left(\alpha_3\beta_1 \sinh(\alpha_4 + \alpha_3(+\mu t + x + y)) + \frac{2\left(\varpi_2^2+\varpi_4^2\right)\varpi_3^2(+\mu t+x+y)}{\varpi_2^2}\right)}{\beta_0 \cos(\alpha_2) + \beta_1 \cosh(\alpha_4 + \alpha_3(+\mu t + x + y)) + \left(\varpi_2 - \frac{\varpi_3\varpi_4(+\mu t+x+y)}{\varpi_2}\right)^2 + (\varpi_3(+\mu t + x + y) + \varpi_4)^2 + \varpi_5}\right]^2. \tag{5.8}$$

$$\mathcal{Q}^{\pm}_{1,1}(x,y,t) = 2\lambda \times \left[\frac{2\left(\alpha_3\beta_1 \sinh(\alpha_4 + \alpha_3(+\mu t + x + y)) + \frac{2\left(\varpi_2^2+\varpi_4^2\right)\varpi_3^2(+\mu t+x+y)}{\varpi_2^2}\right)}{\beta_0 \cos(\alpha_2) + \beta_1 \cosh(\alpha_4 + \alpha_3(+\mu t + x + y)) + \left(\varpi_2 - \frac{\varpi_3\varpi_4(+\mu t+x+y)}{\varpi_2}\right)^2 + (\varpi_3(+\mu t + x + y) + \varpi_4)^2 + \varpi_5}\right]^2. \tag{5.9}$$

5.2. HB

We use the following test function for attaining the HB wave solution:

$$f = \beta_1 e^{(q(\alpha_3\zeta+\alpha_4))} + e^{(-q(\alpha_1\zeta+\alpha_2))} + \beta_0 \cos(q_1(\alpha_5\zeta + \alpha_6)), \tag{5.10}$$

where $\alpha_i (i = 1, 2, \cdots, 6)$ are constants. Inserting Eqs (5.10) into (5.2) and taking coefficients hyperbolic and exponential functions to zero with similar powers and hence on proceeding with mathematica, we get

Set-1. When

$$\left\{\alpha_3 \to -\alpha_1 + \frac{i\sqrt[6]{2}\sqrt[3]{\kappa_3}}{q},\ \beta_0 \to 0,\ \kappa_1 \to -\frac{\sqrt[3]{\kappa_3}}{\sqrt[3]{2}},\ \kappa_2 \to 2^{2/3}\sqrt[3]{\kappa_3}\right\}, \tag{5.11}$$

via the above values, we get

$$f = e^{-q(\alpha_1\zeta+\alpha_2)}\left(1+\beta_1 e^{\sqrt[6]{2}i\zeta\sqrt[3]{\kappa_3}+\alpha_2 q+\alpha_4 q}\right). \tag{5.12}$$

Thus,

$$\mathcal{P} = -2\alpha_1 q + \frac{2i\sqrt[6]{2}\beta_1\sqrt[3]{\kappa_3}e^{\sqrt[6]{2}i\zeta\sqrt[3]{\kappa_3}+\alpha_2 q+\alpha_4 q}}{1+\beta_1 e^{\sqrt[6]{2}i\zeta\sqrt[3]{\kappa_3}+\alpha_2 q+\alpha_4 q}}, \tag{5.13}$$

and by imposing Eq (5.13), we get the following solutions:
Cluster 2:

$$\mathcal{N}^{\pm}_{1,2}(x,y,t) = \left[-2\alpha_1 q + \frac{2i\sqrt[6]{2}\beta_1\sqrt[3]{\kappa_3}e^{\alpha_2 q+\alpha_4 q+\sqrt[6]{2}i\sqrt[3]{\kappa_3}(+\mu t+x+y)}}{1+\beta_1 e^{\alpha_2 q+\alpha_4 q+\sqrt[6]{2}i\sqrt[3]{\kappa_3}(+\mu t+x+y)}}\right]\times e^{i\kappa_3 t-\frac{i\sqrt[3]{\kappa_3}(x-2y)}{\sqrt[3]{2}}}. \tag{5.14}$$

$$\mathcal{H}^{\pm}_{1,2}(x,y,t) = 2\lambda(\kappa_2+\kappa_1)\times\left[-2\alpha_1 q + \frac{2i\sqrt[6]{2}\beta_1\sqrt[3]{\kappa_3}e^{\alpha_2 q+\alpha_4 q+\sqrt[6]{2}i\sqrt[3]{\kappa_3}(+\mu t+x+y)}}{1+\beta_1 e^{\alpha_2 q+\alpha_4 q+\sqrt[6]{2}i\sqrt[3]{\kappa_3}(+\mu t+x+y)}}\right]^2. \tag{5.15}$$

$$\mathcal{Q}^{\pm}_{1,2}(x,y,t) = 2\lambda\times\left[-2\alpha_1 q + \frac{2i\sqrt[6]{2}\beta_1\sqrt[3]{\kappa_3}e^{\alpha_2 q+\alpha_4 q+\sqrt[6]{2}i\sqrt[3]{\kappa_3}(+\mu t+x+y)}}{1+\beta_1 e^{\alpha_2 q+\alpha_4 q+\sqrt[6]{2}i\sqrt[3]{\kappa_3}(+\mu t+x+y)}}\right]^2. \tag{5.16}$$

5.3. Evaluation of M-shape solitons

We assume the following test function for achieving the M-shape wave solution:

$$f = (\alpha_1\zeta+\alpha_2)^2 + (\alpha_3\zeta+\alpha_4)^2 + \alpha_5, \tag{5.17}$$

where $\alpha_i (i = 1, 2, \cdots, 5)$ are constants. Inserting Eqs (5.17) into (5.2) and taking coefficients ζ to zero with similar powers and hence on proceeding with mathematica, we get
Set-1. When

$$\left\{\alpha_5 \to -\frac{(\alpha_2\alpha_3-\alpha_1\alpha_4)^2}{\alpha_1^2+\alpha_3^2},\ \lambda \to -\frac{1}{16},\ \kappa_3 \to \kappa_1^2\kappa_2\right\}, \tag{5.18}$$

via the above values, we get

$$f = (\alpha_1\zeta+\alpha_2)^2 + (\alpha_3\zeta+\alpha_4)^2 - \frac{(\alpha_2\alpha_3-\alpha_1\alpha_4)^2}{\alpha_1^2+\alpha_3^2}. \tag{5.19}$$

Thus,

$$\mathcal{P} = \frac{4\left(\alpha_1^2+\alpha_3^2\right)}{\alpha_1^2\zeta+\alpha_3(\alpha_3\zeta+\alpha_4)+\alpha_2\alpha_1}, \tag{5.20}$$

and by imposing Eq (5.20), we get the following solutions:
Cluster 3:

$$\mathcal{N}^{\pm}_{1,3}(x,y,t) = \left[\frac{4\left(\alpha_1^2+\alpha_3^2\right)}{\alpha_2\alpha_1+\alpha_1^2(+\mu t+x+y)+\alpha_3(\alpha_4+\alpha_3(+\mu t+x+y))}\right]\times e^{i\left(\kappa_2\kappa_1^2 t+\kappa_1 x+\kappa_2 y\right)}. \tag{5.21}$$

$$\mathcal{H}^{\pm}_{1,3}(x,y,t) = 2\lambda(\kappa_2+\kappa_1)\times\left[\frac{4\left(\alpha_1^2+\alpha_3^2\right)}{\alpha_2\alpha_1+\alpha_1^2(+\mu t+x+y)+\alpha_3\left(\alpha_4+\alpha_3(+\mu t+x+y)\right)}\right]^2. \quad (5.22)$$

$$Q^{\pm}_{1,3}(x,y,t) = 2\lambda\times\left[\frac{4\left(\alpha_1^2+\alpha_3^2\right)}{\alpha_2\alpha_1+\alpha_1^2(+\mu t+x+y)+\alpha_3\left(\alpha_4+\alpha_3(+\mu t+x+y)\right)}\right]^2. \quad (5.23)$$

5.4. Cross-kink rational wave solution

We construct the following test function for obtaining the cross kink rational wave solution:

$$f = \alpha_1 e^{(\zeta\varrho_1+\varrho_2)} + e^{(-(\zeta\varrho_1+\varrho_2))} + (\zeta\varpi_1+\varpi_2)^2 + (\zeta\varpi_3+\varpi_4)^2 + \varpi_5, \quad (5.24)$$

where $\varrho_1,\ \varrho_2$, and $\varpi_i,\ i = 1,\cdots,5$ are constants. Inserting Eqs (5.24) into (5.2) and taking coefficients exponential and ζ to zero with similar powers and hence on proceeding with mathematica, we get
Set-1. When

$$\left\{\varrho_1\to 0,\ \varpi_1\to i\varpi_3,\ \varpi_5\to\frac{\left(\kappa_2^{3/2}-2\sqrt{\kappa_3}\right)(4\lambda+1)(\varpi_2-i\varpi_4)^3}{3\sqrt{\kappa_3}\varpi_2},\ \alpha_1\to 0,\ \kappa_1\to-\frac{\sqrt{\kappa_3}}{\sqrt{\kappa_2}}\right\}, \quad (5.25)$$

via the above values, we get

$$f = (\varpi_2+i\zeta\varpi_3)^2 + (\zeta\varpi_3+\varpi_4)^2 + \frac{\left(\kappa_2^{3/2}-2\sqrt{\kappa_3}\right)(4\lambda+1)(\varpi_2-i\varpi_4)^3}{3\sqrt{\kappa_3}\varpi_2} + e^{-\varrho_2}. \quad (5.26)$$

Thus,

$$\mathcal{P} = \frac{4\varpi_3(\varpi_4+i\varpi_2)}{(\varpi_2+i\zeta\varpi_3)^2+(\zeta\varpi_3+\varpi_4)^2+\frac{\left(\kappa_2^{3/2}-2\sqrt{\kappa_3}\right)(4\lambda+1)(\varpi_2-i\varpi_4)^3}{3\sqrt{\kappa_3}\varpi_2}+e^{-\varrho_2}}, \quad (5.27)$$

and by imposing Eq (5.27), we get the following solutions:
Cluster 4:

$$\mathcal{N}^{\pm}_{1,4}(x,y,t) = \left[\frac{4\varpi_3(\varpi_4+i\varpi_2)}{\frac{\left(\kappa_2^{3/2}-2\sqrt{\kappa_3}\right)(4\lambda+1)(\varpi_2-i\varpi_4)^3}{3\sqrt{\kappa_3}\varpi_2}+(\varpi_2+i\varpi_3(+\mu t+x+y))^2+(\varpi_3(+\mu t+x+y)+\varpi_4)^2+e^{-\varrho_2}}\right]\times e^{i\left(\kappa_3 t-\frac{\sqrt{\kappa_3}x}{\sqrt{\kappa_2}}+\kappa_2 y\right)}. \quad (5.28)$$

$$\mathcal{H}^{\pm}_{1,4}(x,y,t) = 2\lambda(\kappa_2+\kappa_1)\times\left[\frac{4\varpi_3(\varpi_4+i\varpi_2)}{\frac{\left(\kappa_2^{3/2}-2\sqrt{\kappa_3}\right)(4\lambda+1)(\varpi_2-i\varpi_4)^3}{3\sqrt{\kappa_3}\varpi_2}+(\varpi_2+i\varpi_3(+\mu t+x+y))^2+(\varpi_3(+\mu t+x+y)+\varpi_4)^2+e^{-\varrho_2}}\right]^2. \quad (5.29)$$

$$Q^{\pm}_{1,4}(x,y,t) = 2\lambda\times\left[\frac{4\varpi_3(\varpi_4+i\varpi_2)}{\frac{\left(\kappa_2^{3/2}-2\sqrt{\kappa_3}\right)(4\lambda+1)(\varpi_2-i\varpi_4)^3}{3\sqrt{\kappa_3}\varpi_2}+(\varpi_2+i\varpi_3(+\mu t+x+y))^2+(\varpi_3(+\mu t+x+y)+\varpi_4)^2+e^{-\varrho_2}}\right]^2. \quad (5.30)$$

5.5. M-Shaped rational wave solution with one kink wave

We construct the following test function for attaining the M-shaped rational wave solution with one kink wave:

$$f = (\zeta\varpi_1+\varpi_2)^2 + (\zeta\varpi_3+\varpi_4)^2 + e^{(\zeta\varpi_6+\varpi_7)} + \varpi_5, \quad (5.31)$$

where $\varpi_i,\ i = 1, \cdots, 7$ are constants. Inserting Eqs (5.31) into (5.2) and taking coefficients exponential and ζ to zero with similar powers and hence on proceeding with mathematica, we get
Set-1. When

$$\left\{\varpi_2 \to -\frac{\varpi_3\varpi_4}{\varpi_1},\ \kappa_1 \to -\frac{\sqrt[3]{\kappa_3}}{\sqrt[3]{2}},\ \kappa_2 \to 2^{2/3}\sqrt[3]{\kappa_3}\right\}, \tag{5.32}$$

via the above values, we get

$$f = \left(\zeta\varpi_1 - \frac{\varpi_3\varpi_4}{\varpi_1}\right)^2 + e^{\zeta\varpi_6+\varpi_7} + (\zeta\varpi_3 + \varpi_4)^2 + \varpi_5. \tag{5.33}$$

Thus,

$$\mathcal{P} = \frac{2\varpi_1^2\left(2\zeta\varpi_1^2 + 2\zeta\varpi_3^2 + \varpi_6 e^{\zeta\varpi_6+\varpi_7}\right)}{\zeta^2\varpi_1^4 + \varpi_1^2\left(\zeta^2\varpi_3^2 + e^{\zeta\varpi_6+\varpi_7} + \varpi_4^2 + \varpi_5\right) + \varpi_3^2\varpi_4^2}, \tag{5.34}$$

and by imposing Eq (5.34), we get the following solutions:
Cluster 4:

$$\mathcal{N}^{\pm}_{1,5}(x,y,t) = \left[\frac{2\varpi_1^2\left(2\varpi_1^2(+\mu t+x+y)+2\varpi_3^2(+\mu t+x+y)+\varpi_6 e^{\varpi_6(+\mu t+x+y)+\varpi_7}\right)}{\varpi_1^4(+\mu t+x+y)^2+\varpi_1^2\left(\varpi_3^2(+\mu t+x+y)^2+e^{\varpi_6(+\mu t+x+y)+\varpi_7}+\varpi_4^2+\varpi_5\right)+\varpi_3^2\varpi_4^2}\right]\times e^{i\kappa_3 t-\frac{i\sqrt[3]{\kappa_3}(x-2y)}{\sqrt[3]{2}}}. \tag{5.35}$$

$$\mathcal{H}^{\pm}_{1,5}(x,y,t) = 2\lambda(\kappa_2+\kappa_1)\times\left[\frac{2\varpi_1^2\left(2\varpi_1^2(+\mu t+x+y)+2\varpi_3^2(+\mu t+x+y)+\varpi_6 e^{\varpi_6(+\mu t+x+y)+\varpi_7}\right)}{\varpi_1^4(+\mu t+x+y)^2+\varpi_1^2\left(\varpi_3^2(+\mu t+x+y)^2+e^{\varpi_6(+\mu t+x+y)+\varpi_7}+\varpi_4^2+\varpi_5\right)+\varpi_3^2\varpi_4^2}\right]^2. \tag{5.36}$$

$$Q^{\pm}_{1,5}(x,y,t) = 2\lambda\times\left[\frac{2\varpi_1^2\left(2\varpi_1^2(+\mu t+x+y)+2\varpi_3^2(+\mu t+x+y)+\varpi_6 e^{\varpi_6(+\mu t+x+y)+\varpi_7}\right)}{\varpi_1^4(+\mu t+x+y)^2+\varpi_1^2\left(\varpi_3^2(+\mu t+x+y)^2+e^{\varpi_6(+\mu t+x+y)+\varpi_7}+\varpi_4^2+\varpi_5\right)+\varpi_3^2\varpi_4^2}\right]^2. \tag{5.37}$$

5.6. Multiwave solution

We formulate the following test function for obtaining double kink interaction with the M-shape solution:

$$f = \beta_1\cos(\zeta\varpi_3+\varpi_4) + \beta_0\cosh(\zeta\varpi_1+\varpi_2) + \beta_2\cosh(\zeta\varpi_5+\varpi_6), \tag{5.38}$$

where $\varpi_i,\ i = 1, \cdots, 6$, are constants. Inserting Eqs (5.38) into (5.2) and taking coefficients trigonometric, hyperbolic and ζ to zero with similar powers and hence on proceeding with mathematica, we get
Set-1. When

$$\left\{\varpi_3 \to \frac{\sqrt{\kappa_3-\kappa_1^2\kappa_2}}{\sqrt{-4\kappa_1-2\kappa_2}},\ \varpi_5 \to \frac{\sqrt{\kappa_3-\kappa_1^2\kappa_2}}{\sqrt{2}\sqrt{2\kappa_1+\kappa_2}},\ \beta_0 =,\ \lambda \to -\frac{1}{4}\right\}, \tag{5.39}$$

via the above values, we get

$$f = \beta_1\cos\left(\frac{\zeta\sqrt{\kappa_3-\kappa_1^2\kappa_2}}{\sqrt{-4\kappa_1-2\kappa_2}}+\varpi_4\right) + \beta_2\cosh\left(\frac{\zeta\sqrt{\kappa_3-\kappa_1^2\kappa_2}}{\sqrt{2}\sqrt{2\kappa_1+\kappa_2}}+\varpi_6\right). \tag{5.40}$$

Thus,

$$\mathcal{P}=\frac{\sqrt{2}\sqrt{\kappa_3-\kappa_1^2\kappa_2}\left(\beta_2\sqrt{-2\kappa_1-\kappa_2}\sinh\left(\frac{\zeta\sqrt{\kappa_3-\kappa_1^2\kappa_2}}{\sqrt{2}\sqrt{2\kappa_1+\kappa_2}}+\varpi_6\right)-\beta_1\sqrt{2\kappa_1+\kappa_2}\sin\left(\frac{\zeta\sqrt{\kappa_3-\kappa_1^2\kappa_2}}{\sqrt{-4\kappa_1-2\kappa_2}}+\varpi_4\right)\right)}{\sqrt{-(2\kappa_1+\kappa_2)^2}\left(\beta_1\cos\left(\frac{\zeta\sqrt{\kappa_3-\kappa_1^2\kappa_2}}{\sqrt{-4\kappa_1-2\kappa_2}}+\varpi_4\right)+\beta_2\cosh\left(\frac{\zeta\sqrt{\kappa_3-\kappa_1^2\kappa_2}}{\sqrt{2}\sqrt{2\kappa_1+\kappa_2}}+\varpi_6\right)\right)},\tag{5.41}$$

and by imposing Eq (5.41), we get the following solutions:

Cluster 6:

$$\mathcal{N}_{1,6}^{\pm}(x,y,t)=\Big[\frac{\sqrt{2}\sqrt{\kappa_3-\kappa_1^2\kappa_2}\left(\beta_2\sqrt{-2\kappa_1-\kappa_2}\sinh\left(\frac{\zeta\sqrt{\kappa_3-\kappa_1^2\kappa_2}}{\sqrt{2}\sqrt{2\kappa_1+\kappa_2}}+\varpi_6\right)-\beta_1\sqrt{2\kappa_1+\kappa_2}\sin\left(\frac{\zeta\sqrt{\kappa_3-\kappa_1^2\kappa_2}}{\sqrt{-4\kappa_1-2\kappa_2}}+\varpi_4\right)\right)}{\sqrt{-(2\kappa_1+\kappa_2)^2}\left(\beta_1\cos\left(\frac{\zeta\sqrt{\kappa_3-\kappa_1^2\kappa_2}}{\sqrt{-4\kappa_1-2\kappa_2}}+\varpi_4\right)+\beta_2\cosh\left(\frac{\zeta\sqrt{\kappa_3-\kappa_1^2\kappa_2}}{\sqrt{2}\sqrt{2\kappa_1+\kappa_2}}+\varpi_6\right)\right)}\Big]\times e^{i\left(\kappa_3 t+\kappa_1 x+\kappa_2 y\right)}.\tag{5.42}$$

$$\mathcal{H}_{1,6}^{\pm}(x,y,t)=2\lambda(\kappa_2+\kappa_1)\times\Big[\frac{\sqrt{2}\sqrt{\kappa_3-\kappa_1^2\kappa_2}\left(\beta_2\sqrt{-2\kappa_1-\kappa_2}\sinh\left(\frac{\zeta\sqrt{\kappa_3-\kappa_1^2\kappa_2}}{\sqrt{2}\sqrt{2\kappa_1+\kappa_2}}+\varpi_6\right)-\beta_1\sqrt{2\kappa_1+\kappa_2}\sin\left(\frac{\zeta\sqrt{\kappa_3-\kappa_1^2\kappa_2}}{\sqrt{-4\kappa_1-2\kappa_2}}+\varpi_4\right)\right)}{\sqrt{-(2\kappa_1+\kappa_2)^2}\left(\beta_1\cos\left(\frac{\zeta\sqrt{\kappa_3-\kappa_1^2\kappa_2}}{\sqrt{-4\kappa_1-2\kappa_2}}+\varpi_4\right)+\beta_2\cosh\left(\frac{\zeta\sqrt{\kappa_3-\kappa_1^2\kappa_2}}{\sqrt{2}\sqrt{2\kappa_1+\kappa_2}}+\varpi_6\right)\right)}\Big]^2.\tag{5.43}$$

$$\mathcal{Q}_{1,6}^{\pm}(x,y,t)=2\lambda\times\Big[\frac{\sqrt{2}\sqrt{\kappa_3-\kappa_1^2\kappa_2}\left(\beta_2\sqrt{-2\kappa_1-\kappa_2}\sinh\left(\frac{\zeta\sqrt{\kappa_3-\kappa_1^2\kappa_2}}{\sqrt{2}\sqrt{2\kappa_1+\kappa_2}}+\varpi_6\right)-\beta_1\sqrt{2\kappa_1+\kappa_2}\sin\left(\frac{\zeta\sqrt{\kappa_3-\kappa_1^2\kappa_2}}{\sqrt{-4\kappa_1-2\kappa_2}}+\varpi_4\right)\right)}{\sqrt{-(2\kappa_1+\kappa_2)^2}\left(\beta_1\cos\left(\frac{\zeta\sqrt{\kappa_3-\kappa_1^2\kappa_2}}{\sqrt{-4\kappa_1-2\kappa_2}}+\varpi_4\right)+\beta_2\cosh\left(\frac{\zeta\sqrt{\kappa_3-\kappa_1^2\kappa_2}}{\sqrt{2}\sqrt{2\kappa_1+\kappa_2}}+\varpi_6\right)\right)}\Big]^2.\tag{5.44}$$

Here, $\zeta=x+y+\mu t$.

6. Dynamical system of the proposed system

The Galilean transformation is a set of equations used in classical mechanics to relate the coordinates of an event in one inertial frame to those in another. This theory, named after physicist Galileo Galilei, describes daily observations at non-relativistic speeds when the relative velocity between two frames is significantly slower than the speed of light. Applying the Galilean transformation to Eq (4.18) yields the dynamical system [41]

$$\begin{cases}\dfrac{d\mathcal{P}}{d\zeta}=\mathcal{W},\\[2ex]\dfrac{dW}{d\zeta}=-\mu_1\mathcal{P}(\zeta)-\mu_2\mathcal{P}^3(\zeta),\end{cases}\tag{6.1}$$

where $\mu_1=\frac{\kappa_3-\kappa_1^2\kappa_2}{2\kappa_1+\kappa_2}$ and $\mu_2=2\lambda$ such that $\kappa_1,\ \kappa_2,\ \kappa_3$, and λ are parameters.

7. The exploration of bifurcation and chaotic dynamics of the proposed system

This section delves further into the bifurcation and chaotic dynamics of the proposed system [42].

7.1. Bifurcation analysis

Here, we analyze the system's bifurcation, which comprises the investigation of phase portraits for the system defined by Eq (4.18). We will resolve the system presented below:

$$\begin{cases}\mathcal{W}=0,\\[2ex]-\mu_1\mathcal{P}(\zeta)-\mu_2\mathcal{P}^3(\zeta)=0.\end{cases}\tag{7.1}$$

The derived equilibrium points (EPs) of system (6.1) are as follows:

$$\zeta_1 = (0, 0), \qquad \zeta_2 = (\sqrt{\frac{i\mu_2}{\mu_1}}, 0), \qquad \zeta_3 = (-i\sqrt{\frac{-\mu_2}{\mu_1}}, 0).$$

The Jacobian for system (6.1) is

$$\mathcal{J}(\mathcal{P}, \mathcal{W}) = \begin{vmatrix} 0 & 1 \\ -\mu_1 - 3\mu_2\mathcal{P}^2 & 0 \end{vmatrix} = -\mu_1 - 3\mu_2\mathcal{P}^2. \tag{7.2}$$

Hence,
•($\mathcal{P}$,0) produces a saddle if $\mathcal{J}(\mathcal{P}, \mathcal{W})) < 0$,
•($\mathcal{P}$,0) produces a center if $\mathcal{J}(\mathcal{P}, \mathcal{W}) > 0$,
• ($\mathcal{P}$,0) produces a cuspidal if $\mathcal{J}(\mathcal{P}, \mathcal{W}) = 0$.

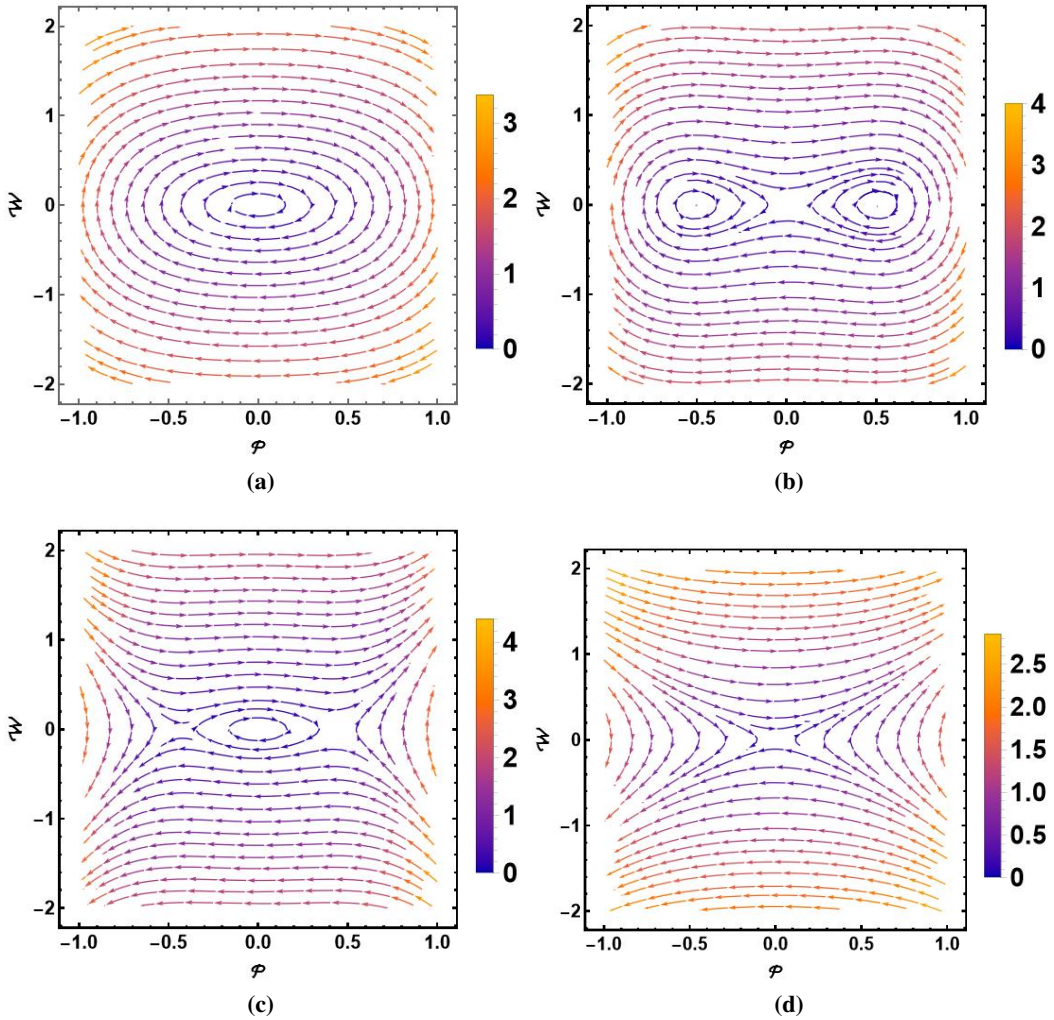

Figure 1. Phase variation plots of the bifurcations of the governed system with arbitrary parameters.

The potential outcomes that can be achieved by modifying the settings are described below.

• **Case-(i)** When $\mu_1 > 0$ and $\mu_2 > 0$, under the parameters $\kappa_1 = -3,\ \kappa_2 = 1,\ \kappa_3 = 1,$ and $\lambda = \frac{1}{3}$, we identify the EP $(0, 0)$. This EP is depicted in Figure 1a, which represents center-like behavior.

• **Case-(ii)** When $\mu_1 > 0$ and $\mu_2 < 0$, under the parameters $\kappa_1 = 0.1,\ \kappa_2 = 0.6,\ \kappa_3 = 3,$ and $\lambda = \frac{-1}{2}$, we identified the EPs, which are $(0, 0),\ (-1, 0)$, and $(1, 0)$. These EPs are visualized in Figure 1b, with (0, 0) characterized as a saddle point, while $(-1, 0)$ and $(1, 0)$ represents center-like behavior.

• **Case-(iii)** When $\mu_1 > 0$ and $\mu_2 < 0$, under the parameters $\kappa_1 = 0.1,\ \kappa_2 = -1,\ \kappa_3 = 3,$ and $\lambda = \frac{2}{3}$, we identified the three EPs $(0, 0),\ (-1, 0)$, and $(1, 0)$. These EPs are demonstrated in Figure 1c, where (0,0) represents center-like behavior, while the remaining two represent the saddle points.

• **Case-(iv)** When $\mu_1 > 0$ & $\mu_2 < 0$, upon applying the parameter values $\kappa_1 = 0.1,\ \kappa_2 = \frac{-1}{2},\ \kappa_3 = 0.3,$ and $\lambda = \frac{-2}{3}$, we find a single point $(0, 0)$. This is visually represented in Figure 1d, where $(0, 0)$ signifies a saddle point.

7.2. Chaotic behavior of the governed system

In the following section, we introduce a perturbation term to investigate the chaotic tendencies of the system described in Eq (6.1). Our analysis encompasses 2D and 3D phase diagrams relevent to this system. We consider the following system:

$$\begin{cases} \frac{d\mathcal{P}}{dt} &= \mathcal{W}(t), \\ \frac{d\mathcal{W}}{dt} &= -\mu_1\mathcal{P}(t) - \mu_2\mathcal{P}^3(t) + \upsilon_1 \sin(\upsilon_2 t), \end{cases} \tag{7.3}$$

For the numerical simulations of both the $\mathcal{W} - \mathcal{P}$ and $\mathcal{W} - \mathcal{P} - t$ phase diagrams of the governed system with parameters $\kappa_1 = 1,\ \kappa_2 = 1,\ \kappa_3 = 1,\ \lambda = .5$, here we take into account two sets of parameter combinations: $[(a), (b)]$ $\upsilon_1 = 1,\ \upsilon_2 = 1$, and $[(c), (d)]$ $\upsilon_1 = .5,\ \upsilon_2 = .1$, as depicted in Figure 2. Additionally, in Figure 3 we exhibit two different sets of frequency and amplitude values: $[(a), (b)]$ $\upsilon_1 = 2.5,\ \upsilon_2 = 1.1$, and $[(c), (d)]$ $\upsilon_1 = 2.1,\ \upsilon_2 = 1.1$, as shown in Figure 2. Figures 2 and 3 illustrate complicated and intriguing behaviors within the phase diagrams, demonstrating the system's sensitivity to perturbations in the parameters υ_1 and υ_2. The system shows a multiscroll pattern and unanticipated dynamics, revealing how the perturbed term $\upsilon_1 \sin(\upsilon_2 t)$ affects the entire system behavior.

Comparing the $\mathcal{P} - \mathcal{W}$ and $\mathcal{P} - \mathcal{W} - t$ phase diagrams under certain parametric values allows for a better awareness of the system's complicated behavior. Such insights are useful for characterizing and predicting the system's response to parameter changes, which has applications in domains such as biology, physics, and engineering.

In Figures 4 and 5, we investigate the dynamics of the perturbed model under different initial conditions. For Figure 4, we used the following parameters: $\kappa_1 = 1,\ \kappa_2 = 1,\ \kappa_3 = 1,\ \lambda = 1.5,\ \upsilon_1 = 4.2$ and $\upsilon_2 = .7$. Also, for Figure 5, the frequency and amplitude values are chosen as $\upsilon_1 = 4.2,\ \upsilon_2 = .7$. We used the following initial conditions for both figures: (a) $[\mathcal{P},\ \mathcal{W}] = [0, 0.5]$, (b) $[\mathcal{P},\ \mathcal{W}] = [0, 0]$, (c) $[\mathcal{P},\ \mathcal{W}] = [0.5, 0]$, and (d) $[\mathcal{P},\ \mathcal{W}] = [0, 0.6]$. The discovery of new attractors enhances our comprehension of the system's complex dynamics.

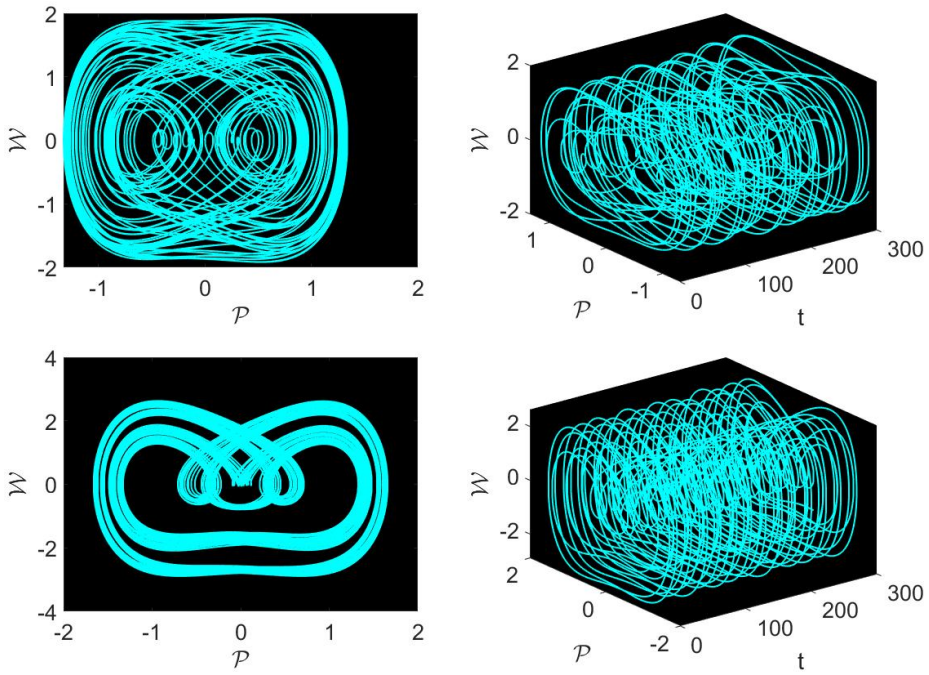

Figure 2. Effects of the initial conditions on the dynamics of system (7.3) with arbitrary parameter values.

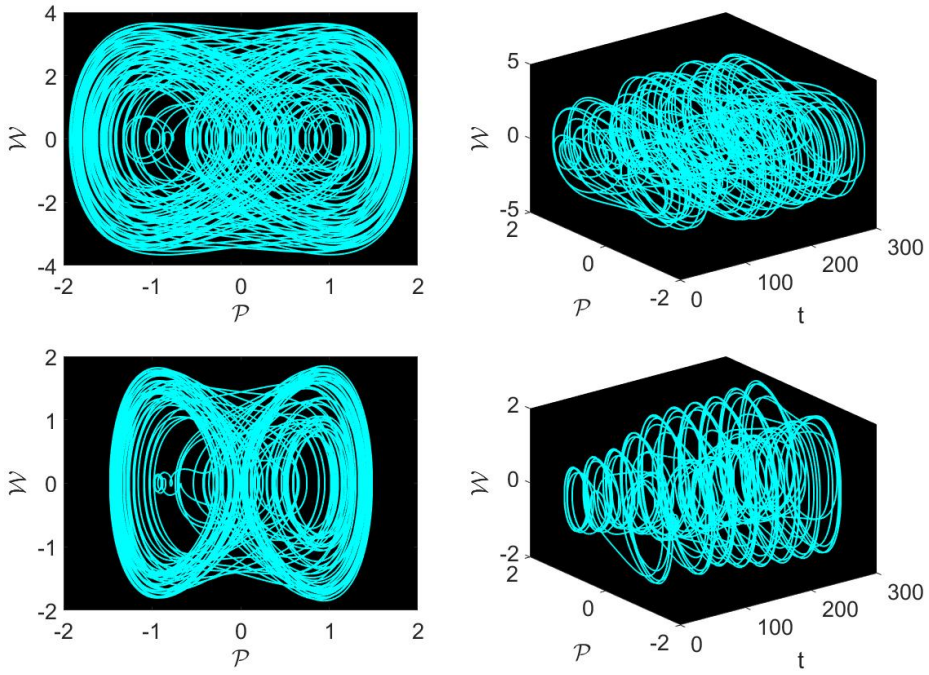

Figure 3. Effects of the initial conditions on the dynamics of system (7.3) with arbitrary parameter values.

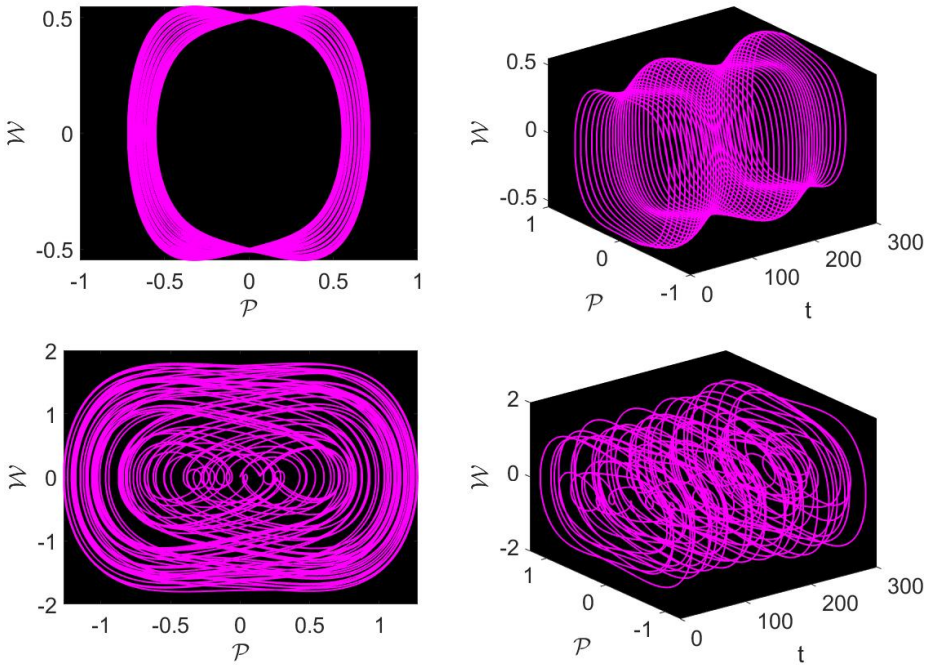

Figure 4. Effects of the initial conditions on the dynamics of system (7.3) with arbitrary parameter values.

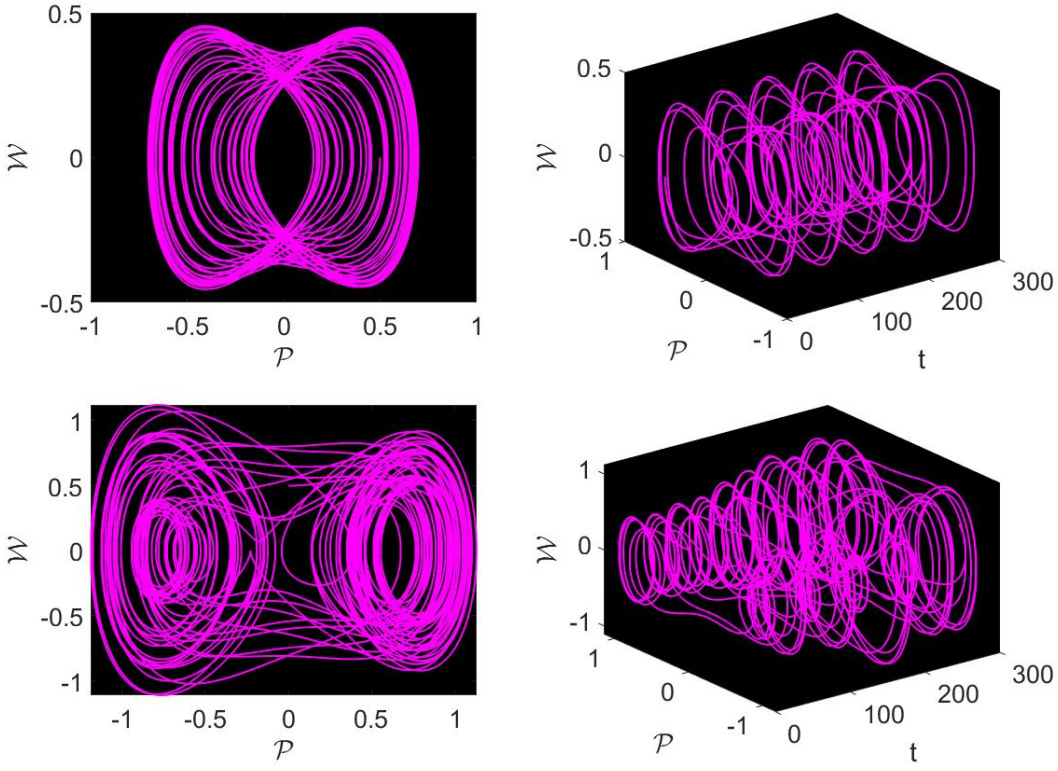

Figure 5. Effects of the initial conditions on the dynamics of system (7.3) with arbitrary parameter values.

8. Results and discussion

In this part, unique contribution is demonstrated by a detailed comparison in contrast of the assessed finding with the previously calculated results. In [33], the (2 + 1)-dimensional CmKDV system was studied by using the Darboux transformation to find soliton solutions. Our work synthesizes this research to apply more effective techniques, namely the AE method and the HB method. Thus, by implementing of the above methodologies, we give novel soliton solutions, such as the bright, dark, combo, periodic, singular, mixed trigonometric, W-M-shape, exponential, hyperbolic, and rational solitary wave solutions, adding complexity to our study. Furthermore, we also find some lump solutions, including the periodic cross rational wave, the HB wave solution, the periodic wave solution, the M-shaped rational wave solution, the M-shaped interaction with one kink wave, and the multiwave solution. These techniques are crucial for producing a variety of soliton structures, as the literature makes clear. Moreover, these techniques are used to generate new soliton wave structures, which improves our research as we investigate the distinct dynamical characteristics and frameworks of soliton solutions. Additionally, the bifurcation analysis of the aforementioned model is also examined, which is especially essential in dynamical systems. Both chaos theory and bifurcation theory are essential tools for understanding complex systems and have widespread applications across various scientific disciplines. This analysis is crucial for understanding the robustness and long-term behavior of solitons in various physical systems. Also, visualizing the solitary wave solutions in various graphical formats is critical for acquiring important physical insights and developing a deeper knowledge of the waveform's structure and dynamics. Here we present some graphs in 3D and 2D, as well as contour plots of the attained solutions in Figures 6–19. These solutions are presented in many dimensions to show how waveforms evolve across time and space, demonstrating their propagation stability. Contour and density plots contribute to elucidating fine details of the solution topology and identifying outlines. The amalgamation of these several graphical representations serves as a significant complement to quantitative analysis, giving researchers a more detailed grasp of solitary wave behavior. The physical interpretation of the analytical sketches as given as follows: In Figure 6, the hyperbolic solution of Eq (4.21) obtained via the AE method is presented using 3D, 2D, and contour plots. Figure 7 showcases $W - M$-shape wave solutions of Eq (4.24), using similar graphical formats. Figure 8 signifies the singular wave solutions of Eq (4.33) by using appropriate parameters. We discovered the periodic behavior of solitons in Figure 9 of Eq (4.36). Figure 10 denotes the combo shape solution of Eq (4.39). Figure 11 illustrates the periodic W-shape solution of Eq (4.42). Figure 12 depicts the dark soliton solutions of Eq (4.51). Figure 13 represents the exponential behavior of Eq (4.57). Figure 14 represents the periodic cross rational behavior of Eq (5.8). Figure 15 shows the HB behavior of Eq (5.15). Figure 16 shows the M-shape behavior of Eq (5.22). Figure 16 illustrates the cross kink rational wave behavior of Eq (5.29). Figure 17 shows the M- shape rational with kink wave behavior of Eq (5.36). Figure 17 represents the multiwave behavior of Eq (5.43). These reported solutions have some physical meaning, for instance dark solitons describe solitary waves with lower intensity than the background. Dark solitons are more difficult to handle than standard solitons, but they have been shown to be more stable and robust to losses. The bright soliton is a soliton whose intensity is higher than the background. There are further types of solitary waves called singular solitons that have singularities, typically with infinite discontinuities. Singular solitons might be linked to solitary waves when the location of the center of the solitary wave is imaginary. Therefore, discussing the

topic of singular solitons is relevant. This type of solution contains spikes and therefore may suggest an explanation for the development of rogue waves. Periodic wave solutions describe waves with a repeating continuous pattern, which determines its wavelength and frequency, while period defines the time required to complete a cycle of waveforms and frequency is a number of cycles per second of time. Periodic solutions in optics form the foundation for understanding and exploiting the periodic nature of light waves, enabling a wide range of applications in science and technology. The kink-type wave solutions are characterized by a sharp transition between two different states, such as a high-density state and a low-density state. The kink itself is a region of rapid change in the wave amplitude, and it propagates through the system at a constant velocity. Homoclinic breather wave solutions are a type of nonlinear wave solution that can arise in certain physical systems. They are characterized by a localized, periodic oscillation that maintains its shape while propagating through the medium. The study confirms that the (2 + 1)-dimensional CmKDV equations can accurately simulate complicated nonlinear dispersive wave phenomena found in modern physics systems.

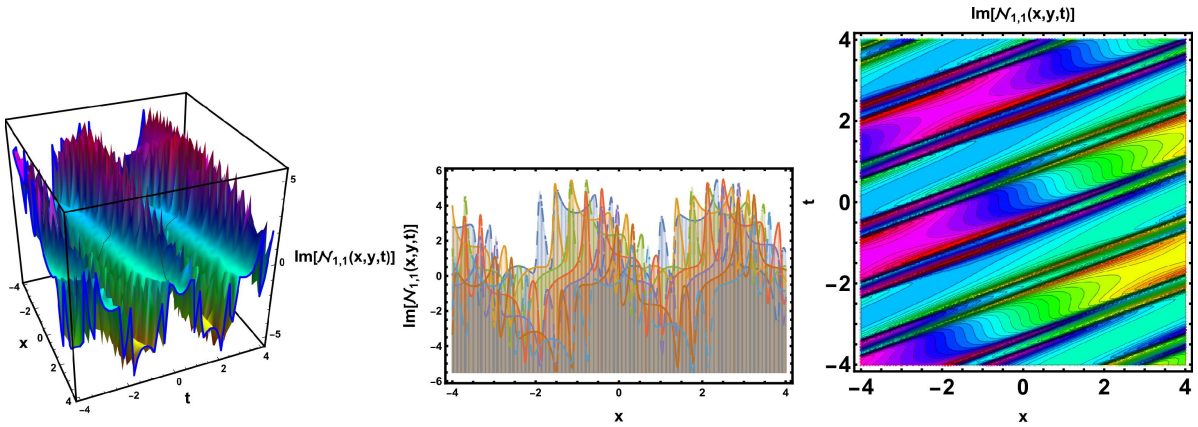

Figure 6. Physical configuration of Eq (4.21) with $\gamma_0 = 2.1$, $\wp_1 = -2.8$, $\wp_2 = -3.1$, $\wp_3 = 0.75$, $\kappa_3 = 0.21$, $\varepsilon = -1$, $\mu = 2.6$, $y = 0.3$.

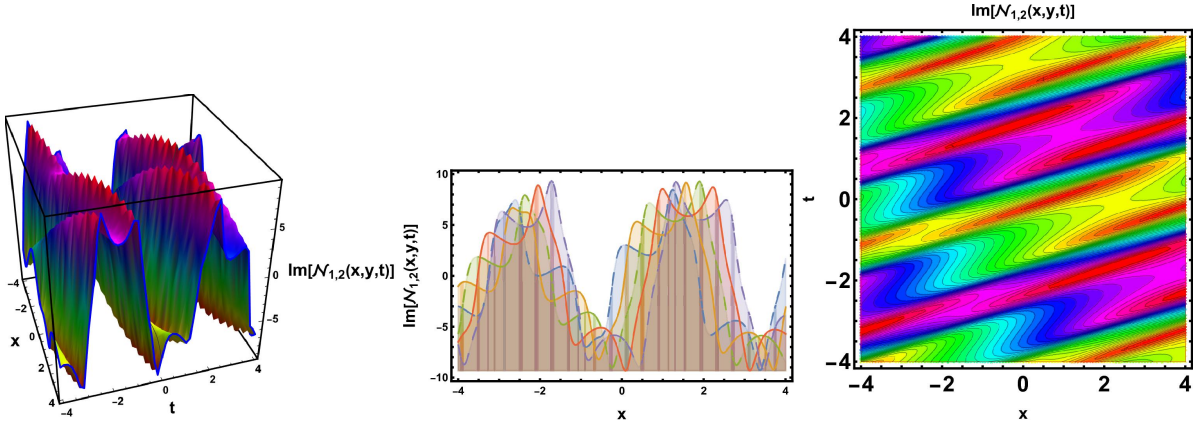

Figure 7. Physical configuration of Eq (4.24) with $\gamma_0 = 2.1$, $\wp_1 = -1.2$, $\wp_2 = 2.01$, $\wp_3 = 2.75$, $\kappa_3 = 1.21$, $\varepsilon = -1$, $\mu = 2.6$, $y = 0.3$.

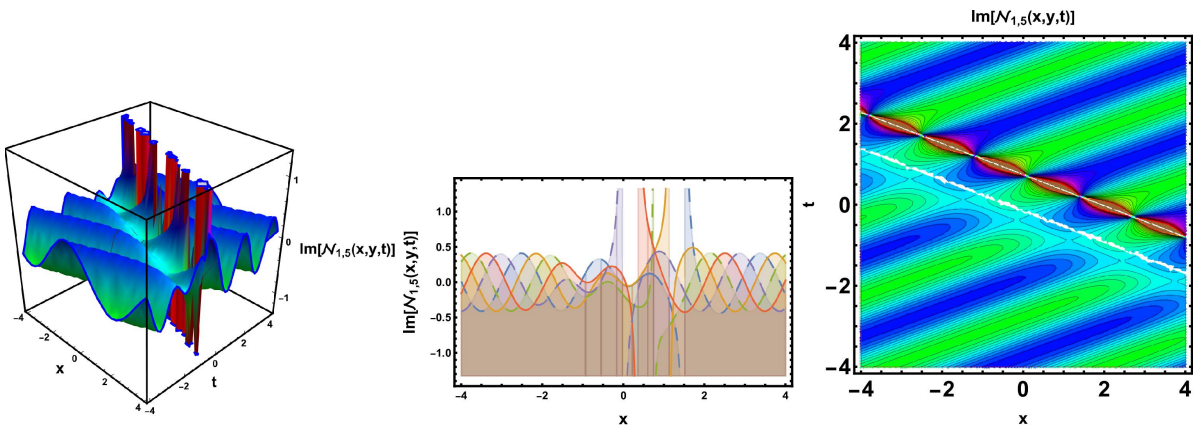

Figure 8. Physical configuration of Eq (4.33) with $\gamma_0 = 0.41$, $\wp_1 = 1.2$, $\wp_2 = 3.1$, $\wp_3 = 2.7$, $\kappa_3 = 3.2$, $\varepsilon = 1$, $\mu = -2.6$, $y = 0.43$.

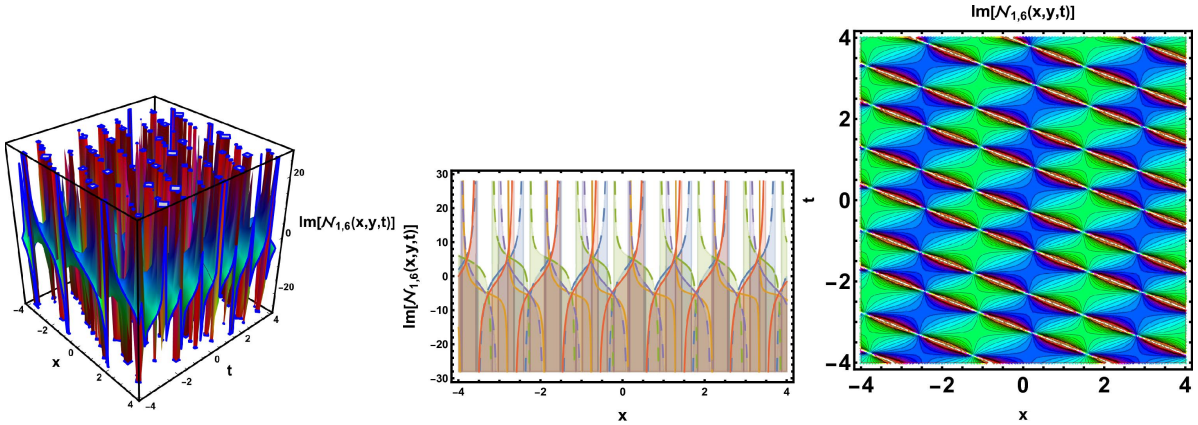

Figure 9. Physical configuration of Eq (4.36) with $\gamma_0 = 0.41$, $\wp_1 = -1.4$, $\wp_2 = 0.2$, $\wp_3 = 0.3$, $\kappa_3 = 3.1$, $\varepsilon = -1$, $\mu = -2.6$, $y = 0.43$.

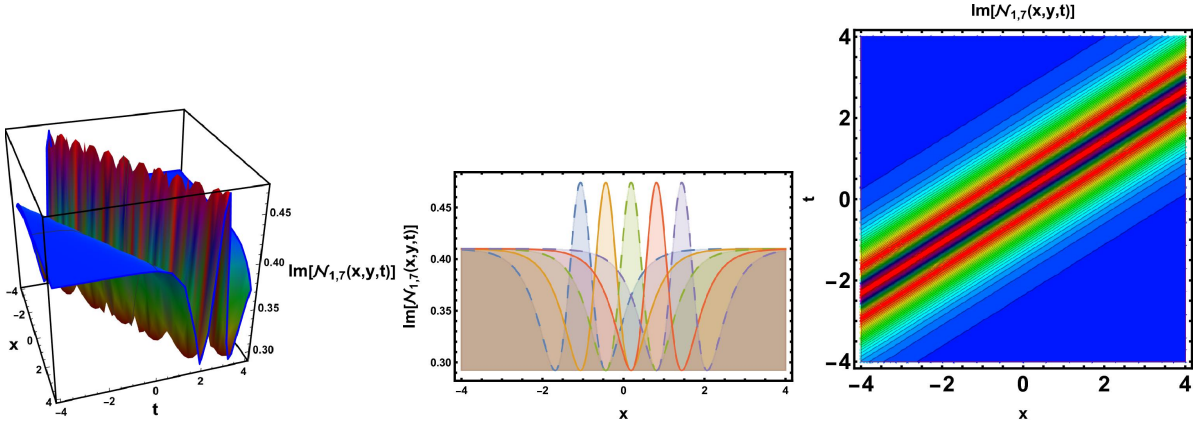

Figure 10. Physical configuration of Eq (4.39) with $\gamma_0 = 0.41$, $\wp_1 = 2.4$, $\wp_2 = 3.2$, $\wp_3 = 2.3$, $\kappa_3 = 1.1$, $\varepsilon = 1$, $\mu = 1.6$, $y = 0.3$.

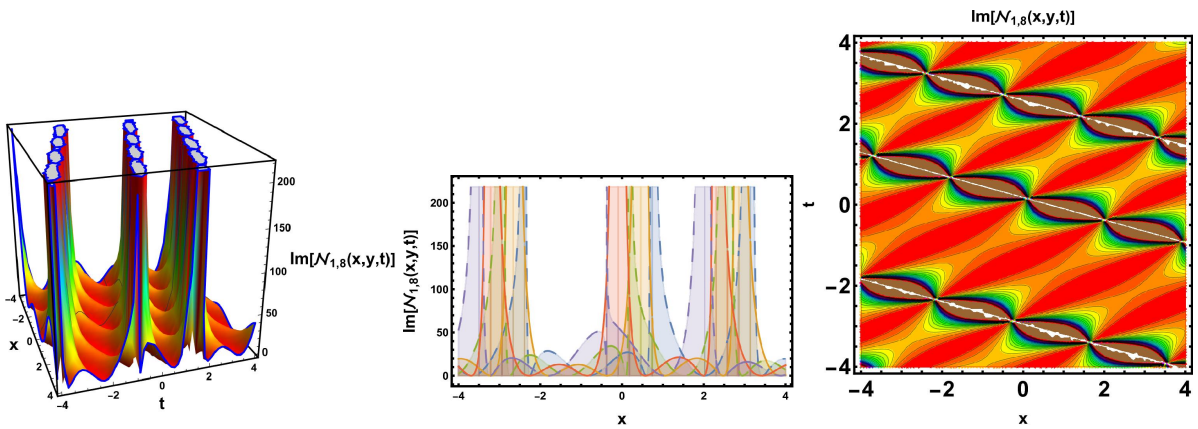

Figure 11. Physical configuration of Eq (4.42) with $\gamma_0 = 0.41,\ \wp_1 = -0.1,\ \wp_2 = 0.2,\ \wp_3 = 2.3,\ \kappa_3 = 2.21,\ \varepsilon = -1,\ \mu = -3.6,\ y = 0.65$.

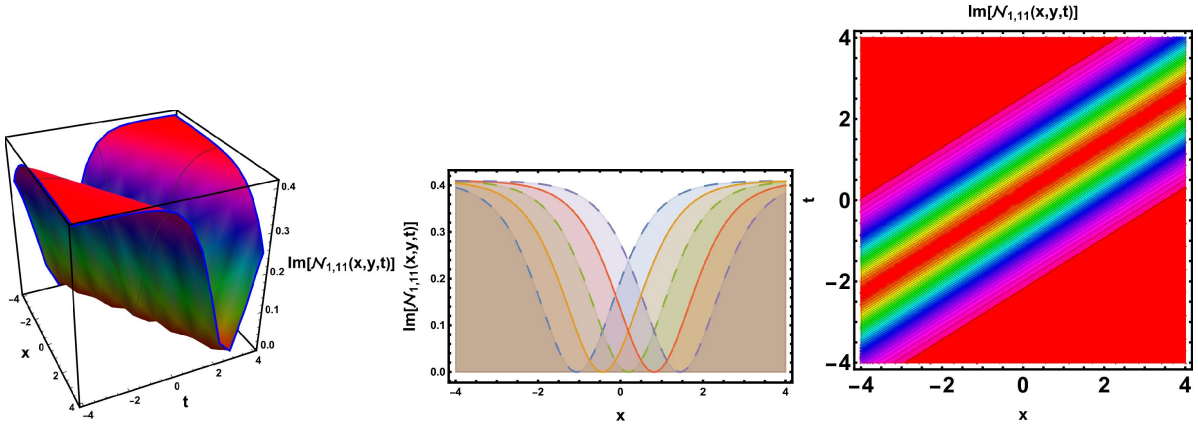

Figure 12. Physical configuration of Eq (4.51) with $\gamma_0 = 0.41,\ \wp_1 = 1,\ \wp_2 = 2,\ \wp_3 = 1,\ \kappa_3 = 1.1,\ \varepsilon = 1,\ \mu = 1.6,\ y = 0.3$.

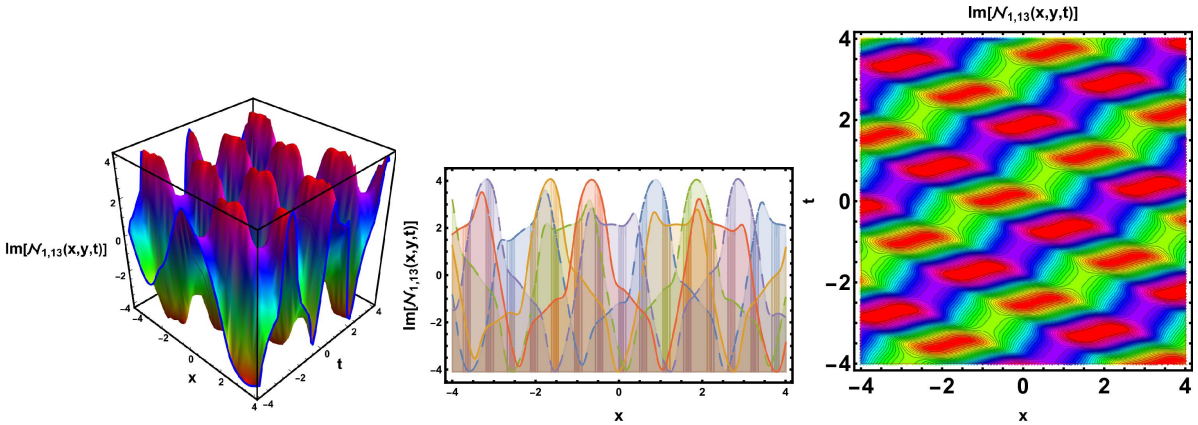

Figure 13. Physical configuration of Eq (4.57) with $\gamma_0 = -3.1,\ \wp_1 = -2.2,\ \wp_2 = -2.4,\ \wp_3 = 3.1,\ \kappa_3 = 2.1,\ \varepsilon = -1,\ \mu = -2,\ y = 0.4$.

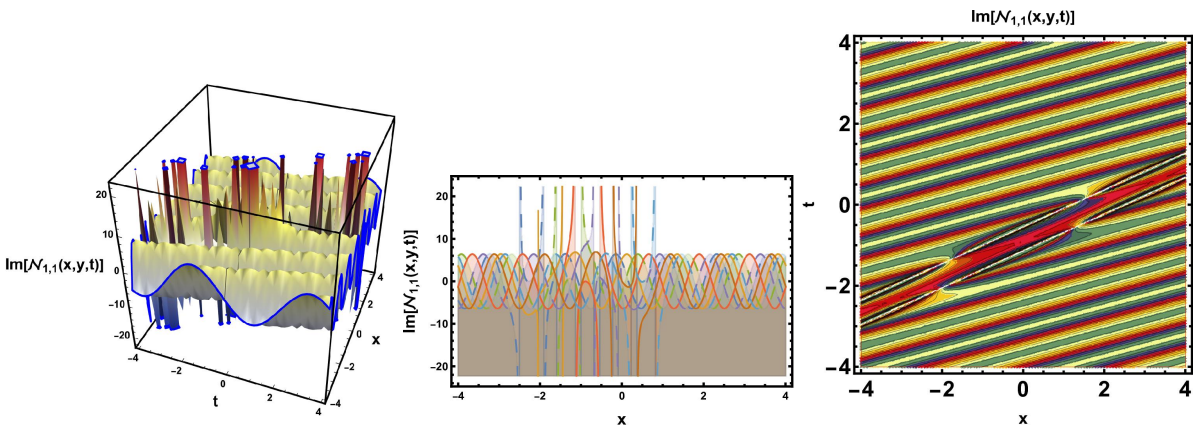

Figure 14. Physical configuration of Eq (5.8) with $\alpha_3 = 3.2$, $\alpha_4 = 0.33$, $\kappa_3 = 5.2$, $\varpi_2 = 0.45$, ‘$\varpi_3 = 0.9$, $\varpi_4 = 0.6$, $\varpi_5 = 0.99$, $\alpha_2 = 0.22$, $\alpha_4 = -7$, $\mu = 2.2$, $\beta_0 = 0.1$, $\beta_1 = -3.2$, $\kappa_3 = 5.1$, $y = 0.5$.

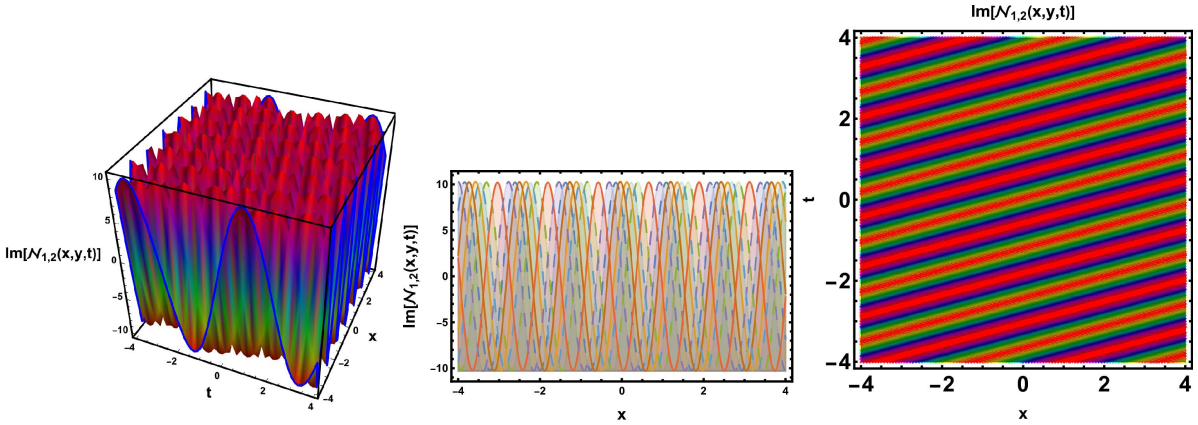

Figure 15. Physical configuration of Eq (5.15) with $q = 2.2$, $\alpha_1 = 2.33$, $\alpha_2 = 4.2$, $\alpha_4 = -7$, $\mu = 0.22$, $\beta_1 = -5.2$, $\kappa_3 = 5.1$, $y = 0.5$.

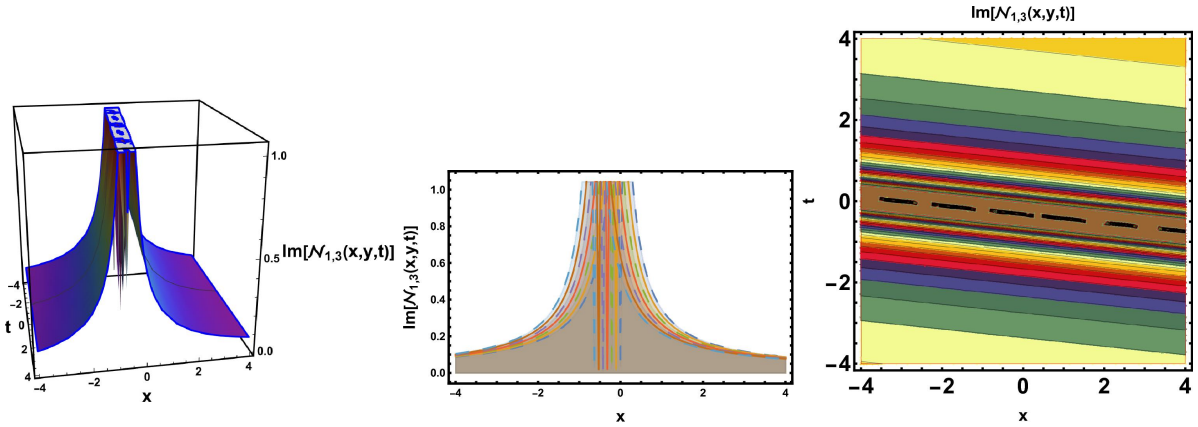

Figure 16. Physical configuration of Eq (5.22) with $\alpha_1 = 0.1$, $\alpha_2 = 0.5$, $\alpha_3 = 2.3$, $\alpha_4 = 3.48$, $\kappa_1 = -2.2$, $\kappa_2 = 0.11$, $y = 0.2$, $\mu = -0.2$.

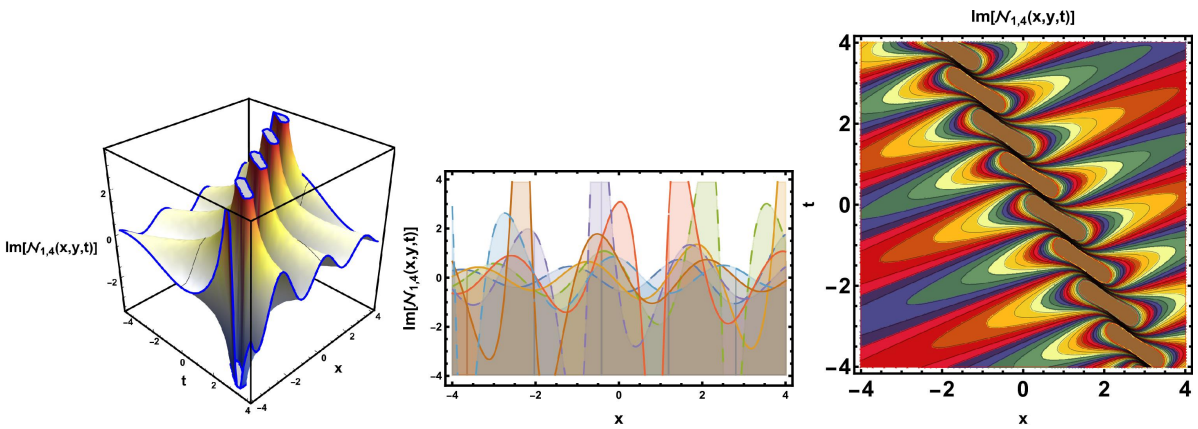

Figure 17. Physical configuration of Eq (5.29) with $\varpi_2 = -5.2$, $\varpi_3 = 8.2$, $\varpi_4 = -7$, $\varrho_2 = 0.22$, $\varrho_3 = -5.2$, $\alpha_1 = 5.1$, $y = -0.6$, $\kappa_1 = 1.5$, $\kappa_2 = 2.7$, ‘$\kappa_3 = 2.4$, $\lambda = 0.19$, $\mu = -0.62$.

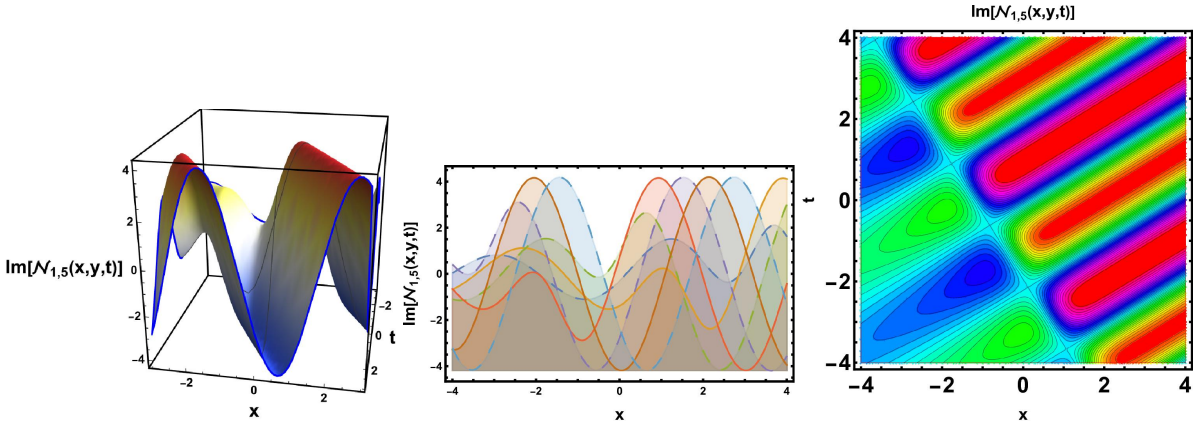

Figure 18. Physical configuration of Eq (5.36) with $\varpi_1 = 3.2$, $\varpi_3 = -2.2$, $\varpi_4 = 2.1$, $\varpi_5 = 2.9$, $\varpi_6 = 2.1$, $\varpi_7 = 5.1$, $y = 0.1$, $\kappa_3 = 1.5$, $\mu = -0.62$.

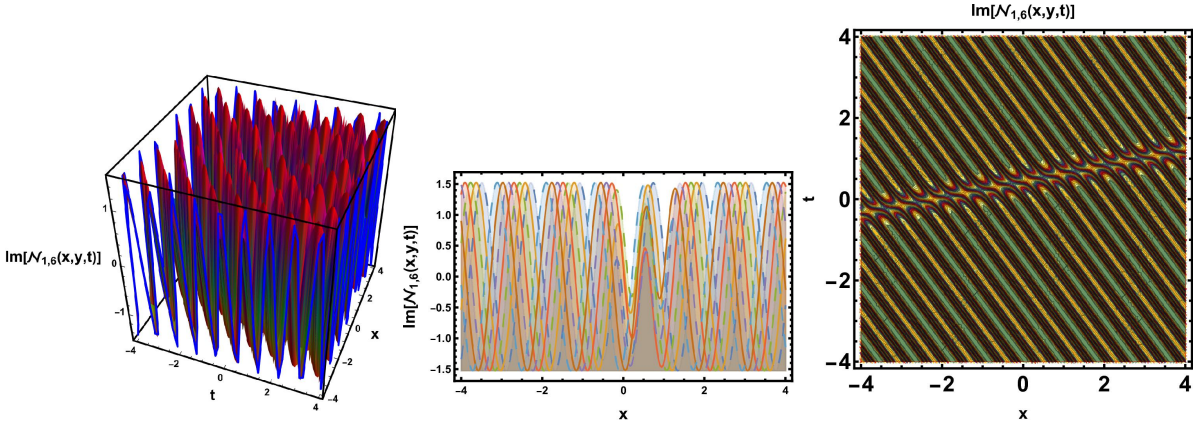

Figure 19. Physical configuration of Eq (5.43) with $\varpi_4 = 0.4$, $\varpi_6 = 2.2$, $\beta_1 = 2.33$, $\beta_2 = 4.2$, $\kappa_1 = -7$, $\kappa_2 = 0.22$, $\kappa_3 = -5.2$, $\mu = 5.1$, $y = 0.5$.

9. Conclusions

In conclusion, this manuscript has offered a through investigation of the (2 + 1)-dimensional CmKDV system, shedding light on its complex dynamics and unveiling a wide array of solitary wave solutions. The features and behavior of the governing model have been illuminated by the underlying methodologies known as the HB method and the AE method. In accordance with the structure of the (2 + 1)-dimensional CmKDV system, we have derived different soliton wave solutions, including dark, bright, singular, periodic, combo, W-shape, trigonometric, hyperbolic, and rational. Additionally, we also found some lump solutions, including the periodic cross rational wave, the HB wave solution, the periodic wave solution, the M-shaped rational wave solution, the M-shaped interaction with one kink wave, and the multiwave solution. Furthermore, we implemented the Galilean transformation to develop a system of ODEs, facilitating a deeper investigation of the system's behavior. Throughout this study, we investigated bifurcations, chaos, and a wide array of other dynamical properties, ultimately providing detailed visualizations of solitary wave solutions. These findings represent a significant advancement in our knowledge of the CmKDV system's complex and frequently unpredictable behavior. It leads readers on an exciting journey into the world of nonlinear waves and dynamical systems, offering additional revelations and insights. As we look ahead, potential pathways for additional inquiry may include a more in-depth examination of the stability and long-term behavior of the identified solitary wave solutions. Moreover, investigating parametric variations and their influence on system dynamics may reveal further intriguing phenomena.

Author contributions

M. A. El-Shorbagy: Formal analysis, Investigation, Writing-original draft; S. Akram: Conceptualization, Methodology, Writing-original draft, Formal analysis, Software; M. ur Rahman: Resources, acquisition, Conceptualization, Writing-review & editing; H. A. Nabwey: Writing-review, Software & editing. All authors have read and approved the final version of the manuscript for publication.

Use of AI tools declaration

The authors declare they have not used Artificial Intelligence (AI) tools in the creation of this article.

Acknowledgments

The authors extend their appreciation to Prince Sattam bin Abdulaziz University for funding this research work through the project number (PSAU/2023/01/29073).

Conflict of interest

The authors declare no conflict of interest.

References

1. S. Akram, J. Ahmad, A. Ali, T. Mohammad, Retrieval of diverse soliton, lump solutions to a dynamical system of the nonlinear (4 + 1) Fokas equation and stability analysis, *Opt. Quant. Electron.*, **55** (2023), 1273. https://doi.org/10.1007/s11082-023-05429-w
2. B. Li, Y. Zhang, X. Li, Z. Eskandari, Q. He, Bifurcation analysis and complex dynamics of a Kopel triopoly model, *J. Comput. Appl. Math.*, **426** (2023), 115089. https://doi.org/10.1016/j.cam.2023.115089
3. B. Li, H. Liang, Q. He, Multiple and generic bifurcation analysis of a discrete Hindmarsh-Rose model, *Chaos Soliton. Fract.*, **146** (2021), 110856. https://doi.org/10.1016/j.chaos.2021.110856
4. X. Zhu, P. Xia, Q. He, Z. Ni, L. Ni, Coke price prediction approach based on dense GRU and opposition-based learning salp swarm algorithm, *Int. J. Bio-Inspir. Com.*, **21** (2023), 106–121. https://doi.org/10.1504/IJBIC.2023.130549
5. X. Zhu, P. Xia, Q. He, Z. Ni, L. Ni, Ensemble classifier design based on perturbation binary Salp swarm algorithm for classification, *Comput. Model. Eng. Sci.*, **135** (2023), 653–671. https://doi.org/10.32604/cmes.2022.022985
6. S. Akram, J. Ahmad, Shafqat-Ur-Rehman, S. Alkarni, N. A. Shah, Analysis of lump solutions and modulation instability to fractional complex Ginzburg–Landau equation arise in optical fibers, *Results Phys.*, **53** (2023), 106991. https://doi.org/10.1016/j.rinp.2023.106991
7. M. S. Ullah, M. Mostafa, M. Z. Ali, H.-O. Roshid, M. Akter, Soliton solutions for the Zoomeron model applying three analytical techniques, *PLoS ONE*, **18** (2023), e0283594. https://doi.org/10.1371/journal.pone.0283594
8. K. J. Wang, Soliton molecules, Y-type soliton and complex multiple soliton solutions to the extended (3 + 1)-dimensional Jimbo-Miwa equation, *Phys. Scr.*, **99** (2024), 015254. https://doi.org/10.1088/1402-4896/ad16fd
9. Y.-H. Yin, X. Lü, R. Jiang, B. Jia, Z. Gao, Kinetic analysis and numerical tests of an adaptive car-following model for real-time traffic in ITS, *Physica A*, **635** (2024), 129494. https://doi.org/10.1016/j.physa.2024.129494
10. Y. Wang, X. Lü, Bäcklund transformation and interaction solutions of a generalized Kadomtsev–Petviashvili equation with variable coefficients, *Chinese J. Phys.*, **89** (2024), 37–45. https://doi.org/10.1016/j.cjph.2023.10.046
11. R. Luo, Rafiullah, H. Emadifar, M. ur Rahman, Bifurcations, chaotic dynamics, sensitivity analysis and some novel optical solitons of the perturbed non-linear Schrödinger equation with Kerr law non-linearity, *Results Phys.*, **54** (2023), 107133. https://doi.org/10.1016/j.rinp.2023.107133
12. I. Onder, A. Secer, M. Ozisik, M. Bayram, Investigation of optical soliton solutions for the perturbed Gerdjikov-Ivanov equation with full-nonlinearity, *Heliyon*, **9** (2023), e13519. https://doi.org/10.1016/j.heliyon.2023.e13519
13. S. Tarla, K. K. Ali, R. Yilmazer, M. S. Osman, On dynamical behavior for optical solitons sustained by the perturbed Chen-Lee-Liu model, *Commun. Theor. Phys*, **74** (2022), 075005. https://doi.org/10.1088/1572-9494/ac75b2

14. S. Sarwar, New soliton wave structures of nonlinear (4 + 1)-dimensional Fokas dynamical model by using different methods, *Alex. Eng. J.*, **60** (2021), 795–803. https://doi.org/10.1016/j.aej.2020.10.009
15. K. S. Nisar, O. A. Ilhan, S. T. Abdulazeez, J. Manafian, S. A. Mohammed, M. S. Osman, Novel multiple soliton solutions for some nonlinear PDEs via multiple Exp-function method, *Results Phys.*, **21** (2021), 103769. https://doi.org/10.1016/j.rinp.2020.103769
16. M. Subasi, H. Durur, Refraction simulation of nonlinear wave for Shallow Water-Like equation, *Celal Bayar University Journal of Science*, **19** (2023), 47–52. https://doi.org/10.18466/cbayarfbe.1145651
17. M. A. El-Shorbagy, S. Akram, M. ur Rahman, Propagation of solitary wave solutions to (4 + 1)-dimensional Davey–Stewartson–Kadomtsev–Petviashvili equation arise in mathematical physics and stability analysis, *Partial Differential Equations in Applied Mathematics*, **10** (2024), 100669. https://doi.org/10.1016/j.padiff.2024.100669
18. S. Akram, J. Ahmad, Shafqat-Ur-Rehman, S. Sarwar, A. Ali, Dynamics of soliton solutions in optical fibers modelled by perturbed nonlinear Schrödinger equation and stability analysis, *Opt. Quant. Electron.*, **55** (2023), 450. https://doi.org/10.1007/s11082-023-04723-x
19. Hamood-Ur-Rehman, M. I. Asjad, M. Inc, T. Iqbal, Exact solutions for new coupled Konno–Oono equation via Sardar subequation method, *Opt. Quant. Electron.*, **54** (2022), 798. https://doi.org/10.1007/s11082-022-04208-3
20. J. Ahmad, S. Akram, S. U. Rehman, N. B. Turki, N. A. Shah, Description of soliton and lump solutions to *M*-truncated stochastic Biswas–Arshed model in optical communication, *Results Phys.*, **51** (2023), 106719. https://doi.org/10.1016/j.rinp.2023.106719
21. J. Ahmad, S. Akram, K. Noor, M. Nadeem, A. Bucur, Y. Alsayaad, Soliton solutions of fractional extended nonlinear Schrödinger equation arising in plasma physics and nonlinear optical fiber, *Sci. Rep.*, **13** (2023), 10877. https://doi.org/10.1038/s41598-023-37757-y
22. S. Gulsen, M. S. Hashemi, R. Alhefthi, M. Inc, H. Bicer, Nonclassical symmetry analysis and heir-equations of forced Burger equation with time variable coefficients, *J. Comput. Appl. Math.*, **42** (2023), 221. https://doi.org/10.1007/s40314-023-02358-y
23. Y. He, L. Zhang, M. S. Tong, Microwave imaging of 3D dielectric-magnetic penetrable objects based on integral equation method, *IEEE Trans. Antenn. Propag.*, **71** (2023), 5110–5120. https://doi.org/10.1109/TAP.2023.3262299
24. Y. Shen, B. Tian, T. Y. Zhou, X. T. Gao, N-fold Darboux transformation and solitonic interactions for the Kraenkel–Manna–Merle system in a saturated ferromagnetic material, *Nonlinear Dyn.*, **111** (2023), 2641–2649. https://doi.org/10.1007/s11071-022-07959-6
25. S.-W. Yao, S. Gulsen, M. S. Hashemi, M. İnç, H. Bicer, Periodic Hunter–Saxton equation parametrized by the speed of the Galilean frame: Its new solutions, Nucci's reduction, first integrals and Lie symmetry reduction, *Results Phys.*, **47** (2023), 106370. https://doi.org/10.1016/j.rinp.2023.106370
26. A. Akbulut, M. Mirzazadeh, M. S. Hashemi, K. Hosseini, S. Salahshour, C. Park, Triki–Biswas model: Its symmetry reduction, Nucci's reduction and conservation laws, *Int. J. Mod. Phys. B*, **37** (2023), 2350063. https://doi.org/10.1142/S0217979223500637

27. Z.-Y. Wang, S.-F. Tian, J. Cheng, The ∂^{-} dressing method and soliton solutions for the three-component coupled Hirota equations, *J. Math. Phys.*, **62** (2021), 093510. https://doi.org/10.1063/5.0046806

28. S.-F. Tian, M.-J. Xu, T.-T. Zhang, A symmetry-preserving difference scheme and analytical solutions of a generalized higher-order beam equation, *Proc. R. Soc. A*, **477** (2021), 20210455. https://doi.org/10.1098/rspa.2021.0455

29. Y. Li, S.-F. Tian, J.-J. Yang, Riemann–Hilbert problem and interactions of solitons in the-component nonlinear Schrödinger equations, *Stud. Appl. Math.*, **148** (2022), 577–605. https://doi.org/10.1111/sapm.12450

30. Z.-Q. Li, S.-F. Tian, J.-J. Yang, On the soliton resolution and the asymptotic stability of N-soliton solution for the Wadati-Konno-Ichikawa equation with finite density initial data in space-time solitonic regions, *Adv. Math.*, **409** (2022), 108639. https://doi.org/10.1016/j.aim.2022.108639

31. M. ur Rahman, M. Sun, S. Boulaaras, D. Baleanu, Bifurcations, chaotic behavior, sensitivity analysis, and various soliton solutions for the extended nonlinear Schrödinger equation, *Bound. Value Probl.*, **2024** (2024), 15. https://doi.org/10.1186/s13661-024-01825-7

32. Z.-Q. Li, S.-F. Tian, J.-J. Yang, E. Fan, Soliton resolution for the complex short pulse equation with weighted Sobolev initial data in space-time solitonic regions, *J. Differ. Equation*, **329** (2022), 31–88. https://doi.org/10.1016/j.jde.2022.05.003

33. R. Myrzakulov, G. Mamyrbekova, G. Nugmanova, M. Lakshmanan, Integrable (2 + 1)-dimensional spin models with self-consistent potentials, *Symmetry*, **7** (2015), 1352–1375. https://doi.org/10.3390/sym7031352

34. K. Yesmakhanova, G. Shaikhova, G. Bekova, R. Myrzakulov, Darboux transformation and soliton solution for the (2 + 1)-dimensional complex modified Korteweg-de Vries equations, *J. Phys.: Conf. Ser.*, **936** (2017), 012045. https://doi.org/10.1088/1742-6596/936/1/012045

35. F. Yuan, X. Zhu, Y. Wang, Deformed solitons of a typical set of (2 + 1)–dimensional complex modified Korteweg–de Vries equations, *Int. J. Appl. Math. Comput. Sci*, **30** (2020), 337–350. https://doi.org/10.34768/amcs-2020-0026

36. F. Yuan, The order-n breather and degenerate breather solutions of the (2 + 1)-dimensional cmKdV equations, *Int. J. Mod. Phys. B*, **35** (2021), 2150053. https://doi.org/10.1142/S0217979221500533

37. G. Shaikhova, N. Serikbayev, K. Yesmakhanova, R. Myrzakulov, Nonlocal complex modified Korteweg-de Vries equations: reductions and exact solutions, In: *Proceedings of the Twenty-First International Conference on Geometry, Integrability and Quantization*, June 3–8, 2019, Varna, Bulgaria, 2020, 265–271. https://doi.org/10.7546/giq-21-2020-265-271

38. A.-M. Wazwaz, The Camassa–Holm–KP equations with compact and noncompact travelling wave solutions, *Appl. Math. Comput.*, **170** (2005), 347–360. https://doi.org/10.1016/j.amc.2004.12.002

39. G. Shaikhova, B. Kutum, R. Myrzakulov, Periodic traveling wave, bright and dark soliton solutions of the (2 + 1)-dimensional complex modified Korteweg-de Vries system of equations by using three different methods, *AIMS Mathematics*, **7** (2022), 18948–18970. http://doi.org/10.3934/math.20221043

40. S. Roy, S. Raut, R. R. Kairi, P. Chatterjee, Bilinear Bäcklund, Lax pairs, breather waves, lump waves and soliton interaction of (2 + 1)-dimensional non-autonomous Kadomtsev–Petviashvili equation, *Nonlinear Dyn.*, **111** (2023), 5721–5741. https://doi.org/10.1007/s11071-022-08126-7

41. I. Alazman, B. S. T. Alkahtani, M. ur Rahman, M. N. Mishra, Nonlinear complex dynamical analysis and solitary waves for the (3 + 1)-D nonlinear extended Quantum Zakharov-Kuznetsov equation, *Results Phys.*, **58** (2024), 107432. https://doi.org/10.1016/j.rinp.2024.107432

42. S. S. Kazmi, A. Jhangeer, N. Raza, H. I. Alrebdi, A.-H. Abdel-Aty, H. Eleuch, The analysis of bifurcation, quasi-periodic and solitons patterns to the new form of the generalized q-deformed Sinh-Gordon equation, *Symmetry*, **15** (2023), 1324. https://doi.org/10.3390/sym15071324

AIMS Press